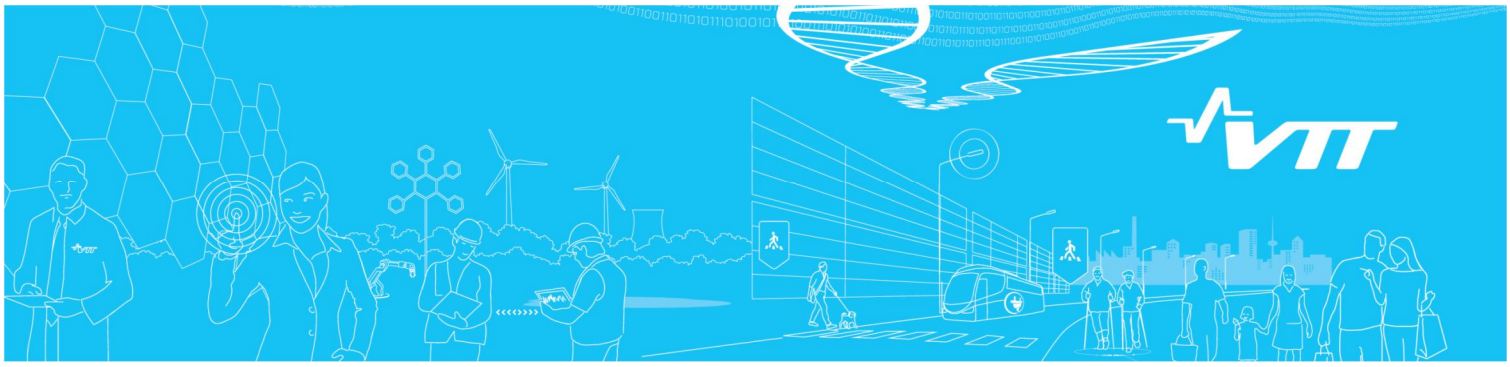

RESEARCH REPORT

VTT-R-04314-14

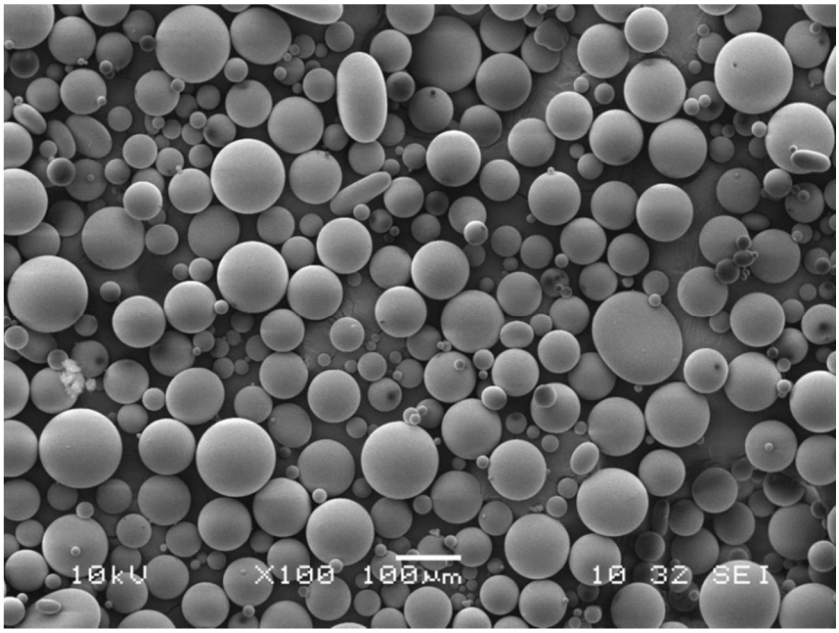

Novel responsive surfaces based on active hybrid coatings utilizing encapsulation technologies

Authors: Juha Nikkola, Sanna Virtanen, Jani Pelto, Tony Munter, Jarmo Ropponen, Johan Mangs and Riitta Mahlberg
VTT Technical Research Centre of Finland (VTT)

Juha Larismaa, Riina Ritasalo, Henrika Granbohm, Outi Söderberg and Simo-Pekka Hannula
Aalto University (Aalto)

Joonas Koivisto and Mirja Kiilunen
Finnish Institute of Occupational Health (FiOH)

Confidentiality: Public

Report's title

Novel Responsive Surfaces based on Active Hybrid Coatings Utilizing Encapsulation Technologies (RESCOAT)

Customer, contact person, address	**Order reference**
Tekes, Ruukki Metals Oy, Fortum Power and Heat Oy, Tikkurila Oyj, Tekno-Forest Oy, Taitotekniikka Oy	40103/11
Project name	**Project number/Short name**
Novel Responsive Surfaces based on Active Hybrid Coatings Utilizing Encapsulation Technologies (RESCOAT)	73055 / RESCOAT
Author(s)	**Pages**
Juha Nikkola, Sanna Virtanen, Jani Pelto, Tony Munter, Jarmo Ropponen, Johan Mangs, Riitta Mahlberg, Juha Larismaa, Qian Chen, Riina Ritasalo, Henrika Granbohm, Outi Söderberg, Simo-Pekka Hannula, Joonas Koivisto and Mirja Kiilunen	40
Keywords	**Report identification code**
Microencapsulation, active coatings, controlled release	VTT-R-04314-14

Summary

RESCOAT project was conducted 1.2.2011 – 31.5.2014 with three research partners (FiOH, Aalto and VTT) and five industrial partners (Fortum, Ruukki Metals, Tikkurila, Taitotekniikka and Tekno-Forest). The project aimed to develop microencapsulation technology for novel active and functional coatings. Microcapsules were aimed to provide added value and new functionalities, such as anti-fouling, self-healing, anti-ice and fire-retardancy.

Both polymeric and ceramic microcapsules were synthesised and characterised. These were implemented into paint and lacquer matrixes. Their performance was demonstrated in accelerated laboratory and field tests. In addition, the safety aspects of the novel coating materials were analysed using particle emission tests.

To summarise the main findings, microencapsulation technology may prolong the usability of anti-fouling coatings. The increase of hydrophilicity in the polymer capsule had evidently effect on the release rate of biocide. Promising self-healing and anti-ice performances were obtained by using polymeric encapsulation technologies. Furthermore, promising coating recipes were developed for fire-retardant (FR) coatings. In addition, the encapsulation of FR materials into silica particles was demonstrated. International collaboration with IST (Lissabon, Portugal) created new know-how regarding to self-healing and corrosion resistant coatings.

Some of the results of RESCOAT project have been highlighted in scientific and technical journals, as well as in conferences and seminars. Besides the major amount of results and data, RESCOAT project has created spin-offs for new Finnish and European research projects.

Confidentiality	Public

Espoo 26.9.2014

Written by	**Reviewed by**	**Accepted by**
Juha Nikkola Senior Scientist	Tarja Laitinen Head of Research Area	Anu Kaukovirta-Norja Vice President, Operations

VTT's contact address

Juha Nikkola, VTT, PL1000, 02044 VTT

Distribution (customer and VTT)

1 original paper copy to Tekes and each project partner: Ruukki Metals Oy, Fortum Power and Heat Oy, Tikkurila Oyj, Tekno-Forest Oy, Taitotekniikka Oy, Aalto, FIOH and VTT.

Preface

The VTT-Aalto-FIOH joint project focused on the development of novel active and responsive surfaces based on hybrid paint and thin coatings with encapsulated active agents. The project was carried out together with three national research institutes and universities (VTT, Aalto and FIOH) in collaboration with five Finnish industrial partners (Fortum, Ruukki Metals, Tikkurila, Teknoforest and Taitotekniikka). The contact persons of the partners and steering group members are presented in Table 1. Dr. Pasi Väisänen (Ruukki Metals) was appointed as chairman of the steering group and respectively, Juha Nikkola (VTT) as secretary. International co-operation was done with Instituto Superior Técnico (IST) (Prof. Maria de Fátima G. da Costa Montemor). Altogether three short-term research visits were conducted from Aalto to IST during the RESCOAT project.

Table 1. List of project partners and their contact persons.

Organisation		**Contact Person**	**Email**
VTT Technical Research Centre of Finland (VTT)	RES	Tarja Laitinen Juha Nikkola (project manager)	Tarja.Laitinen@vtt.fi Juha.Nikkola@vtt.fi
Aalto University – School of Chemical Technology (Aalto)	UNI	Simo-Pekka Hannula	Simo-Pekka.Hannula@aalto.fi
Finnish Institute of Occupational Health, (FIOH)	OTH	Mirja Kiilunen	Mirja.Kiilunen@ttl.fi
Fortum Oyj	IND	Ritva Korhonen	Ritva.Korhonen@fortum.com
Ruukki Metals Oy	IND	Pasi Väisänen	Pasi.Vaisanen@ruukki.com
Tikkurila Oyj	IND	Ilkka Vehmaan-Kreula	Ilkka.Vehmaan-Kreula@tikkurila.com
Taitotekniikka Oy	SME	Pasi Makkonen	Pasi.Makkonen@taitotekniikka.fi
Tekno-Forest Oy	SME	Tomi Pohjolainen	Tomi.Pohjolainen@pineline.fi

The authors would like to acknowledge the financial support of Tekes, Fortum, Ruukki Metals, Tikkurila, Taitotekniikka, Tekno-Forest, FiOH, Aalto and VTT. In addition, all researchers and technicians are acknowledged for their skilful and efficient work.

Espoo 26.9.2014

Authors

Contents

1. Introduction

RESCOAT project focused on the development of novel active and responsive surfaces based on hybrid paint and thin coatings with encapsulated active agents. The developed polymeric or silica capsules were either slowly releasing or responsive to the external stimulus. The active agents in the capsules had different functionalities being e.g. flame retardants, biocides, self-healers, antifreezers. By combining and further developing the existing know-how of hybrid coating and encapsulation technologies, the project aimed to provide feasible functional solutions against biofouling, delayed flare-up, or ice nucleation.

Anti-fouling

External surfaces of buildings and transportation as well as safety electronic devices are continuously exposed to various harmful agents, e.g. soiling. Biofouling – settlement of biofilm and micro-organisms on material surfaces – leads to large financial losses by causing aesthetic detriments, corrosion damages, and malfunction of the components, for example in underwater cooling systems. Traditionally used toxic protection material organo-tin (TBT) is nowadays banned worldwide. Recently, anti-fouling has been tried to overcome by preventing the adhesion of organisms to coatings by modification of their surface structure or chemistry, or by utilization of natural anti-fouling compounds in them. However, efficient and ecological solutions for biofouling are still lacking.

Fire-retardant

The novel constructions made of steel – especially of thin sheet material – must meet tight requirements, which include also the longer resistance for fire. The major problem arises from the impairment of the mechanical properties of the structure as temperature rises. Therefore, retardation of the heating of the steel is important. One aspect in improving the performance is to apply a coating that delays the heat conduction. So, if the steel sheet as such reaches the critical temperature within 15 minutes (the standard class R15, ISO 834), it may be that with a suitable coating this can be improved up to 30 min (R30). In order to decrease the heat conduction of the coating FRs should be incorporated into the layer. With our approach of application of encapsulation techniques the amount of the reactive agents can be kept smaller than in layer-by-layer solutions.

Self-healing

Self-healing functionality can be targeted to prevent crack propagation, to patch shallow defects on the material surface for aesthetic reasons, or to seal the defected surface from getting exposed to environmental factors (moisture, oxygen etc.). Microencapsulation techniques are feasible in this functionality, and they have been used for example in scratch resistant coatings for cars, where the paint automatically repairs the minor surface damages, while the heating causes coating to flow into the scratch. Scratches in the coatings during transport and storage cause large material losses.

Anti-ice

Ice layers at technical surfaces are a big challenge in cold climate regions causing safety risks and damages. The operation breaks caused by them lead to major problems in transportation, power generation, etc. At the moment there is severe need for novel anti-ice treatments which replace or complement the existing thermal, chemical or mechanical methods.

2. Goal

The RESCOAT project aimed to produce responsive and active surfaces by developing hybrid coating structures via encapsulation technologies (Figure 1). The main objective of the project was to study responsive coating material solutions for anti-fouling, fire-retardant, self-healing, and anti-ice applications.

The main development and production targets of the RESCOAT project were:

- To develop responsive microencapsules to be used in paints and hybrid thin coatings
- To study the trigger release of the active agents implemented into microencapsules
- To select and develop suitable materials for the active agent and the capsule shell in order to provide desired release of the active agent in different matrices
- To incorporate the developed microencapsules into coating matrices
- To verify the performance and service life of the coatings with the microcapsules
- To evaluate environmental aspects of the developed responsive surfaces by conducting life cycle analyses (LCA)
- To demonstrate and test the usability of the novel responsive coating combinations in different exterior applications

New types of responsive coatings with tailored properties were aimed to create by combining paints or sol-gel coatings with encapsulated agents released in a controlled way. The development of microcapsules providing the desired functionality was targeted in the project. The fabrication of the most suitable capsules was up-scaled so that there was enough material for the implementation to the test coatings. Behaviour of the new responsive coatings was tested both at the laboratory scale and accelerated tests before the demonstration in larger scale.

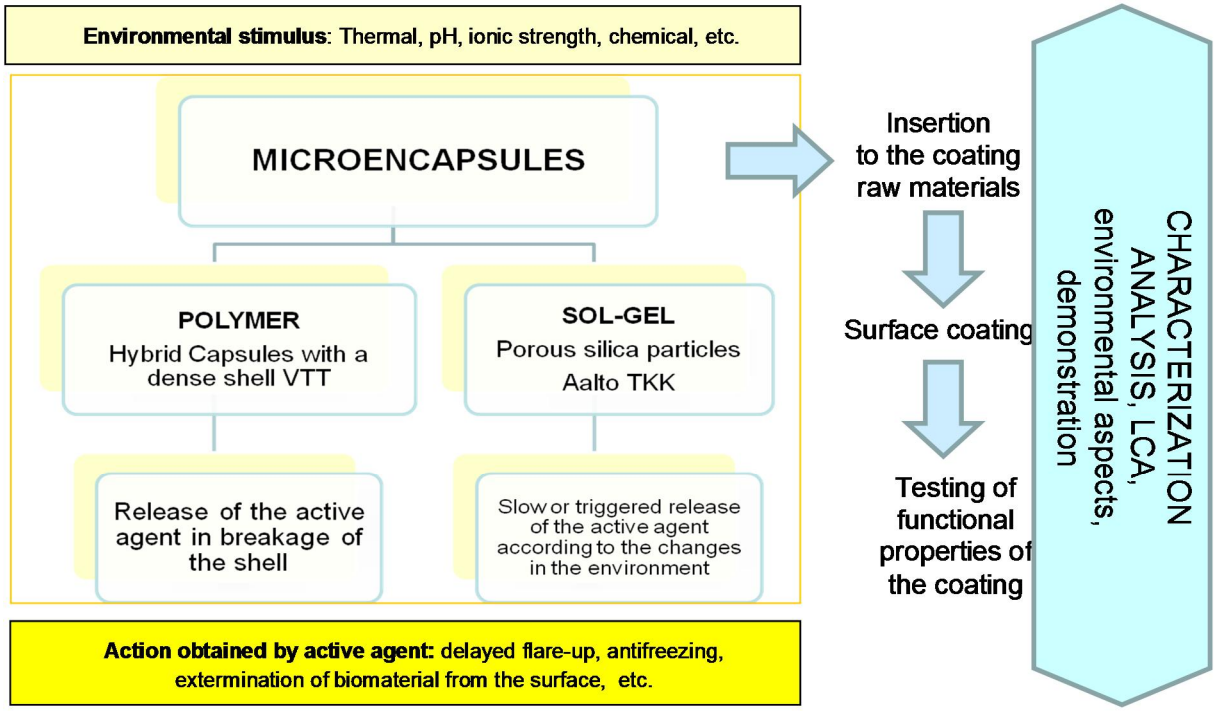

Figure 1. The different techniques, actions, and targets in the RESCOAT project.

3. State-of-the-art

Adaptive and active coatings can be best defined as coatings that offer both functionality and design, so as to respond to any environmental/internal influence or impact. Applying small containers with diameters of 0.1-100 µm for the responsive controlled release of the active compounds, has been successfully used by pharmaceutical in drug delivery systems (DDS), foods, cosmetics, agrochemical, and textile industry [1,2]. These concepts and technologies have not been used at their fully potential in some application areas where they could have a lot to offer. Demands for surfaces with targeted functionality are increasing and, thus, there is a need for different responsive controlled release solutions. Tailored release systems reacting on demand and providing the desired functionality face the challenges set by the service conditions, environmental consciousness, and legislation.

The environmental stimuli, such as heat, chemical reactions, moisture, pH, pressure, electrical or magnetic field etc. causes different kinds of alterations to take place in an active and adaptive coating. For example the stimuli can cause the active chromatic dyes to change their colour, which can be applied for indicative condition monitoring, as made in the spoilage indicators of active packaging [3]. The changes can be also reversible as in active textiles providing information of the physiological changes of the wearer. In the fire-fighting sector, thermochromic dyes have been engineered to change the protective clothing to white under extreme temperatures in order to reflect the heat away from the body [4].

3.1 Anti-fouling surfaces

According to existing knowledge marine biofouling takes place in four steps: 1) formation of an organic film when organic molecules or possibly inorganic compounds are accumulated on the substrate, 2) settlement of bacteria and single-cell diatoms (primary colonizers), 3) settlement of algal spores, barnacle cyprids, marine fungi etc. (secondary colonizers), and 4) growth of larger marine micro-organisms such as macroalgae (tertiary colonizers) [5]. Signals related to the compounds or metabolites of the organisms occurring in these different phases can be considered as triggering agents for the stimuli-responsive systems. Physical factors such as flow rate or water temperature may be function as triggers, as well.

Due to the European BPD and VOC directives there are major challenges to obtain sufficient protection for biofouling. Annually the consequences of biological fouling in marine and freshwater environments costs are over $ 15 billion per year [6], and those caused by the surface damages by moisture and biocontaminants are over 30 billion euros merely in Europe. The previously used toxic antifouling materials, such as organo-tin (TBT), are today prohibited. Currently, the control of living organisms such as fungus or algae consists of adding large enough amount of the fungicide to the paint, which has both the environmental and efficiency problems. When added to the coatings this way, the biocides may dissolve in the service environment, which reduces the coating efficacy and leads to even larger additions of active agents. This has driven to seek eco-efficient anti-fouling solutions, and thus, non-biocidic approaches such as surface nanostructuring have been studied to prevent the adhesion of marine organisms. However, nanostructuring does not alone prevent sufficiently biofouling, and therefore, also natural biocides, ultra-smooth non-stick coatings, acoustic pulsing (e.g. by means of piezoelectric coatings), or chlorine gas generated through

[1] Ahn BY, Seok SI, Bai IC. Sol–gel microencapsulation of hydrophilic active compounds from the modified silicon alkoxides: The control of pore and particle size, Mat. Sci. Eng. C 28 (2008) 1183–1188.
[2] Wang SB, Ordered mesoporous materials for drug delivery, Microporous and Mesoporous Materials 117 (2009) 1–9.
[3] Kruijf N, Beest M, Rijk R, Sipiläinen-Malm T, Losada P, Meulenaer B, Active and intelligent packaking: applications and regulatory aspects. Food Add. Contam. 19 (2002), 144-162.
[4] Tang S, Stylios G: An overview of smart technologies for clothing design and engineering. IJCST 2006.
[5] Yebra, D., Kiil, S. & Dam-Johansen, K. Antifouling technology - past, present and future steps towards efficient and environmentally friendly antifouling coatings, Progress in Organic Coatings, 50 (2004) 75-104.
[6] www.ambio.bham.ac.uk

electronic action have been used [7]. So far, they have not been any practical breakthroughs. Therefore, more targeted protection is needed for the long-term antifouling/preservation. Some slow release anti-fouling coatings based on encapsulated active agents have been launched to markets and are promised to provide long-term performance in marine applications [8]. The slow release may be obtained through different approaches e.g. through nanosized antifouling agents which are explained to stay long in the coating lattices, due to slow self-polishing action of the coating matrix leading to release of the antifoulant or due to binding the active agents to less soluble compounds. Recently, stimuli responsive surfaces with encapsulated activates have shown potential to provide the control of surface contamination. As the active agent is released only when a contaminant is detected, the amount of active agents in the coating is retained at the level that ensures functionality of the structure for longer time. The functional hypothesis is that when the surface is contaminated its properties change and the stimuli responsive capsules containing active agents react and release the biocides.

VTT and the Department of Chemistry at the University of Helsinki have studied star-or hyperbranched amphiphilic polymers as carriers for active agents in view of preserving wood against fungi. The first feasibility study (2005–2006) concerned the use of synthetic smart polymers for building materials [9]. The basic innovative research *Functional Surfaces with Encapsulated Activates Designed for Wood-based Materials* (FUNCAP) was funded by the Academy of Finland 2008-2010. Its focus is to understand the basic phenomena occurring during biological contamination of wood as well as to design and to synthesize various types of polymer capsules into which fungicides are encapsulated to be released by external stimuli. In addition, the release was found to be dependent on the structural properties of the polymer and the fungicide [10].

Antibacterial properties can be obtained also by using such additives as silver in the coatings. Then the bacterial population is not directly killed, but their reproduction is stopped. This has been studied at AALTO in the DONAMO project *Protective materials modified with the doped sol-gel nanoparticles* (2007-2009, funded by Tekes and consortium of Finnish companies) [11,12]. The controlled release of silver is a relevant factor for the life time of the functional surface, and here, the hollow silica capsules with controlled pore size could be feasible [13,14].

[7] Brizzolara RA, Nordham DJ, Walch M, Lennen RM, Simmons R, Burnett E, Mazzola MS, Non-chemical biofouling control in heat exchangers and seawater piping systems usin acoustic pulses generated by an electrical discharge. Biofouling, 1(2003), 19-35.
[8] http://www.microteklabs.com/paintcoat.html
[9] Jämsä S, Ritschkoff A, Posti O, Salparanta L, Löija M, Paavilainen J, Mahlberg R, Viitanen H, Tenhu H, Määttä P, Älypolymeerit ja rakennustuotteiden kestävyyys - Smartdur. Tekes-loppuraportti. 30.6.2006. Confidental.
[10] Jämsä, S., Mahlberg, R., Ritschkoff, A.-C. & Tenhu, H. Effect of active agents released from poly(acrylic acid) matrices on mold resistance, submitted to Wood Material Science and Engineering
[11] Jasiorski M, Skoczylas A, Hermanowicz K, Haimann K, Strek W, Maruszewski K, Surface-Enhanced Raman Spectra of Substances Adsorbed on Ag^0 Clusters Deposited on SiO_2 Submicron Spheres Prepared by the Sol-Gel Method, Opt. Mat. 26 (2004) 145-149.
[12] Larismaa L, Söderberg O, Ge Y, Liu XW, Honkanen T, Laine J, Friman M, Kolari M, Vuorio T, Väisänen P, Juhanoja J, Rosenberg M, Alanen A, Hannula S-P, Effect of annealing on the morphology of Ag-doped submicron silica powder prepared via modified Stöber method, 5th Int. Conf. Sol-Gel Mat, Trzebieszowice, Poland, 1-5.6.2008.
[13] Andersson J, Areva S, Spliethoff B, Lindén M, Sol-gel synthesis of a multifunctional, hierarchically porous silica/apatite composite. Biomat. 26 (2005) 6827-6835.
[14] Czuryszkiewicz T, Areva S, Honkanen M, Lindén M, Synthesis of sol-gel silica materials providing a slow release of biphosphonate. Coll. Surf. A 254 (2005) 69-74.

3.2 Fire-retardant surfaces

Fire resistance is defined as the time during which a structural element can withstand fire exposure as imposed to a standard fire test [15,16]. There are three major functionalities that have relevance during the first steps of a fire: (I) the thermally insulating construction prevents the increase of temperature on the other side of the wall, (E) the construction should maintain its integrity, and (R) the construction should bear loads [17]. The fire retardant (FR) prevents the fire or retards its growth and spread, i.e. flash over, by controlling the fire properties of combustible items. It reduces also the smoke development.

In constructions the lightweight unprotected steel parts may fail after 5-10 min exposure to an intense fire. The critical temperature region starts at 390 – 470 ^{o}C depending on the steel grade, the design of the construction [18], and the coatings applied. In standard ISO 834 the steel structures are divided into classes 15, 30, 60, 90, 120, 180, and 240 min depending on time needed to reach the critical temperature. This moment is delayed by a shielding FR layer that retards heat convection to the steel. In order to design feasible FR encapsulation, the possible triggers are the increase of temperature or CO content. The common optical fire alarm apparatus are calibrated to the infrared emissions of CO2 band at 4.4 µm [19]. Gas detection has been demonstrated also with the doped sol-gel silica films [20]. However, the most feasible trigger in the present case is the temperature rise.

Flame retardants are classified to additive and reactive FR's. Additive FR's are usually mineral fillers, hybrids or organic compounds, such as silica, talc, calcium carbonate, and glass fibers [21]. The active FR's can act physically (cooling, diluting the fuel gases, forming a protective layer), or by chemically (reacting in the condensed or gas phase) [22]. In the first case the additives in the flame retardant decompose consuming heat (endothermic reaction) and cool the reaction medium. Such are some metal hydroxides liberating water vapour at approx. 200-300^{o}C, and additives that release specific radicals which react with the highly reactive species (such as H• and OH•) forming less reactive or inert polymer molecules. Decomposing FR may form also inert gases and thus dilute the combustible gas mixture. Some FR additives form a protective layer between the gaseous phase (combustion) and the solid phase (thermal degradation). This layer limits or prohibits the transfer of combustible volatile gases and oxygen, which prevents the combustion process.

Partly the same idea is applied in FR's where a thick shielding layer is created on the surface as the fire starts. This is called intumescing, i.e. the protective material swells into solid, insulating foam when the flame reaches it. For example, in the white Muralo Fire Retardant latex Flat Paint intumescing results in a black foam layer - the paint consists of 9.2 % pigments (titania, silicates), 90.8 % carriers (vinyl/acetate acrylic resin, melamine resin, dipentaerythritol), and 23.9 % active agent (ammonium phosphate) [23]. This composition includes actually several of the most applied FR's – such as brominated FR's, phosphorus FR's, APP's, melamine based FR's, and metal hydroxides. The brominated FR's have been used widely, but their use is currently becoming more restricted due to environmental and health issues, though they are used in brominated vegetable oils. However, other FR's are becoming more common. Rigid PU foam is used in insulation panels as well as the organic

[15] Zalosh RQ: Industrial fire protection engineering, Wiley, 2003
[16] E1 Suomen rakentamismääräyskokoelma Rakennusten paloturvallisuus Määräykset ja ohjeet 2002, Ympäristöministeriön asetus rakennusten paloturvallisuudesta, 39 s.
[17] http://www.specialchem4polymers.com/tc/flame-retardants/index.aspx?id=9318
[18] ECCS No 89 ECCS Tekninen komitea 3 – Teräsrakenteiden palonkestävyys (mitoituslaskenta), Teräsrakenneyhdistys ry., 6 p.
[19] Nolan DP, Handbook of fire and explosion detection engineering for Oil, Gas, Chemical and Related Facilities, Noyes publications, 1996, 291 p.
[20] Della Gaspera E, Buso D, Guglielmi M, Martucci A, Bello V, Mattei G, Post ML, Cantalini C, Agnoli S, Granozzi G, Sadek AZ, Kalantar-Zadeh K, Wlodarski W, Comparison study of conductometric, optical and SAW gas sensors based on porous sol-gel silica films doped with NiO and Au nanocrystals, Sens. Act. B 143 (2010) 567-573.
[21] http://www.cheshireribbon.co.uk
[22] Laoutid F, Bonnaud L, Alexandre M, Lopez Cuesta JM, Dubois Ph, New prospects in flame retardant polymer materials: From fundamentals to nanocomposites, Mat. Sci. Eng. R 63 (2009) 100125.
[23] http://d0server1.fnal.gov/users/bagby/www/L1_Cal/ORC_Docs/paint_msds.pdf

phosphorus compounds (phosphates, phosphonates). Also, Ammonium Polyphosphate (APP) may be used with in many different polyurethane (PU) applications, and with Polyethylene / Polypropylene (PE/PP). One fast growing segment in the markets are the melamine based FR's (pure melamine, melamine borate, melamine phosphate, melamine polyphosphate, melamine cyanurate), and metal hydroxides (aluminium trihydroxide (ATH), magnesium dihydroxide (MDH)). For example, melamine infers to the combustion process in all its stages: at about 350^{o}C melamine salt sublimates to pure melamine causing a heat sink and retarding the ignition of fire; melamine vaporization at higher temperature uses heat and delays the combustion, nitrogen formed in this reaction acts as inert diluents together with ammonia, and the char layer forms a barrier between oxygen and the polymeric decomposition gases.

3.3 Anti-ice surfaces

Ice forms when water droplets impinge on a surface below 0°C. Here, the kinetics influences: the ice formation is the slower, the quicker the water droplet rolls off the surface and the slower it freezes to ice. Also, surface chemistry and topography can affect the process. The higher is the water contact angle, the easier it rolls off the surface. Thus, a superhydrophobic coating should perform well as an anti-ice surface which has already demonstrated [24]. The nanostructured hydrophilic/hydrophobic surface layers are also expected to provide retardation of ice formation and growth.

There are three growth types of ice: (i) frozen droplets merge laterally forming larger ice nucleus on the surface; (ii) a thin ice layer grows in thickness; and (iii) ice needles grow by condensation. High water contact angle prevents two separate droplets grow together. This is obtained with superhydrophobicity by surface chemistry and topography. Their influence on the ice growth from a thin ice layer is not yet known. Surface energy has retards the ice growth by condensation [25].

Chemical composition of the coating and physicochemical properties of the coating surface are responsible for the hydrophobic and cold properties of the coating at the liquid-solid interface. The adhesion to ice of the most polymer materials is higher than 0.1 MPa. One way to control the icing is to use in the coatings such polymers in which the critical surface tension of wetting σ_{cr} < 25 N/m, and the contact angle for water > 90°, so that the adhesion strength of ice to the surface is < 0.03 MPa [26]. Examples of these are poly(tetrafluoroethylene) (PTFE or Teflon®) and poly(dimethylsiloxane) (silicone or PDMS) [27 28 29]. Other coatings with high hydrophobicity, low ice-adhesion, and suitable other properties can be prepared from organo-silicon polymers, such as epoxy-silicone (Wearlon®). Its ice adhesion is reduced with factor of about 12 when compared to aluminium reference, while the respective value for Teflon® is about 2 [30]. Other possibilities have been obtained by mixing polysiloxane and fluorocarbons; for example, polyperfluoalkyl-methacrylate modified with a lithium compound reduces ice adhesion by a factor 25 when compared to PTFE.

Overall, the anti-icing coatings should combine seemingly incompatible properties, such as the high adhesion to the protected surface and the minimum adhesion to the ice. For

[24] Wang et al. Cold Regions Sci. Technol. 62 (2010) 29.
[25] Na, Webb, Int. J. Heat Mass Transfer 46 (2003) 3797.
[26] Chuppina SV, Anti-Icing gradient organosilicate coatings. Glass Phys. Chem. 33 (2007) 502–509.
[27] Mulherin ND, Haehnel RB, Progress in evaluating surface coatings for icing control at corps hydraulic structures. Ice Eng., Technical Note 2003, 03–4.
[28] Frankenstein S, Tuthill AM, Ice adhesion to locks and dams: Past work; future directions. J. Cold Regions Eng. 16 (2002) 83–96.
[29] Croutch VK, Hartley RA, Adhesion of ice to coatings and the performance of ice release coatings. J. Coat. Techn. 64 (1992) 41–53.
[30] Laforte C, Beisswenger A, Icephobic Material Centrifuge Adhesion Test. Proc 11th Int. Workshop Atmospheric Icing of Structures, Montréal, 2005, 1–6.

atmospheric ice, the problems could partly be solved by the above mentioned coatings. However, the lifetime, mechanical and anti-adhesion stability of the current materials are not satisfying. At certain super-cooling conditions, strong icing still occurs on these surfaces destroying the icephobicity. Thus, the prevention of ice accretion on surfaces is still under investigation. A realistic goal is the production of durable, industrially-viable coatings with reduced ice adhesion forces. In addition development of the superhydrophobic (passive acting) coatings, the focus is changing to the active anti-ice coatings, for example such that are working on a biomimetic coating concept or biochemical method [31].

Table 2. Commercial icephobic coatings [32 33 34 35 36 37].

Company	Product name	Compositions
KissCote, Inc. (USA)	MegaGuard, LiquiCote	Polydimethyl siloxane used on aluminum samples and painted steel
Microphase Coatings (USA)	Phasebreak B-2	Epoxy polymers, silicate mesh, and new melt-point-depressants for military use
S&A Fernandina, Inc. (USA)	RIP-4004	Saturated polyester resins modified with fluorotelomer intermediates activated with a biuret of HDI.
21st Century Coatings, Inc. (USA)	Urethane-51PC951	A fluorinated polyurethane coating, suitable for both in-air and in-water immersion.
NuSil Technology (USA)	R-2180	A two-part silicone elastomer dispersed in xylene.
Ameron International Protective Coatings Group (USA)	PSX-700	Siloxane and polyurethane epoxy.
Troy Corporation (USA)	TroyGuard	Fluoropolymer suspension and mineral spirits in clear acrylic urethane paint.
Ecological Coatings (USA)	3000 series	No details.
Indmar Coatings Corporation (USA)	V-766E	Vinyl resin, titanium dioxide and carbon black, diisodecyl phthalate, methyl isobutyl ketone, toluene ortho phosphoric acid
	V-102e	Vinyl resin, aluminum powder diisodecyl phthalate, methyl isobutyl ketone, toluene

3.4 Microencapsulation techniques

Microencapsulation is one of the quality preservation techniques of sensitive substances and a good method for production of materials with novel properties. In microencapsulation the micron-sized particles are enclosed in a shell. In the present project the shell is either polymeric or of silica. The different microencapsulation techniques can be roughly divided into the chemical and physical encapsulation [38]. In chemical process a dispersed phase (e.g. organic solvent or silica) containing the encapsulation material and the active agent are mixed with an anti-solvent (e.g. water) to form an emulsion or a suspension (oil-in-water), which upon polymerization leads to the formation of capsules or microspheres. Some of the physical encapsulation techniques include coacervation and phase separation techniques, layer-by-layer (LbL) assembly of electrically charged particles (polyelectrolyte), spray-drying method, and sol-gel encapsulation technique [38]. Which microencapsulation technique is chosen depends on the core or encapsulation material used and its properties, such as viscosity, solubility, etc., and on the desired properties of the microcapsules (e.g. particle size). The factors influencing to core and shell are given in Table 3.

[31] IFAM Jahresbericht 2008/2009
[32] Progress in Evaluating Surface Coatings for Icing Control at Corps Hydraulic Structures. U.S. Army Eng. Res. Dev. Center, Hanover, NH. October 2003.
[33] Ice engineering. Chapter 20. Control of Icing on Hydraulic Structures. EM 1110-2-1612 . September 2006.
[34] Chuppina SV, Anti-Icing Gradient Organosilicate Coatings. Glass Phys. Chem. 33 (2007) 502–509.
[35] Burkitt B, Riegler B, Thomaier R, Sivas S, Hoover K, Silicone coatings for aircraft. Nusil Silicone Technology. September 25, 2007.
[36] http://www.ecologicalcoatings.com/icephobic.html
[37] http://www.sti.nasa.gov/tto/spinoff1996/67.html
[38] Ghosh SW, in Functional Coatings by Polymer Microencapsulation, ed.Ghosh SW, Wiley-VCH, Weinheim, 2006, pp. 15-23

Table 3. Microcapsule core and shell [39,40,41,42,43].

Categories	Core	Shell
Material	Active chemicals such as organics, organometallics, proteins, enzymes, etc. in the form of solution, dispersion or emulsion.	Natural or man-made polymers providing permeable, semi-permeable, or impermeable properties.
Function	Function of core materials varies with required applications.	(i) Permeable shells are used for release applications; (ii) Semi-permeable capsules are impermeable to the core material, but permeable to low molecular-weight liquids; (iii) The impermeable shell encloses the core material and protects it from the external environment.
Critical factors	(i) Compatibility of the core materials with the shell; (ii) Size of the core particles is essential for diffusion, permeability or controlled release applications.	(i) Compatibility of the shell with the core material; (ii) Thickness and pore size of the permeable shell wall controls the release of the core material.

Porous silica particles

Silica is applied as a shell material to obtain the controlled release of the active agent, and thus, the release speed can be controlled, for example, with the pore size of the porous shell. The hollow and porous silica particles can be made with oil-in-water method, by exploiting evaporating inner polymer shell under the silica, or by applying porous polymer coating of silica and targeted etching [44,45].

The silica encapsulation has been used for the carriers of the hydrophilic active compounds, in magnetic luminescent nanocomposite particles [46], in the photocatalytic active adsorbent [47]. The capsules can be tailored by the various core materials, by the size of the silica particles and their surface chemistry, by the added inorganic or organic adhering components or even by fabricating multicomponent nanocomposites [48,49,50]. With a multilayer structure the correct environmental trigger can be selected [51]. Capsules can be guided also by the magnetic field, if they include magnetic dopants [52,53].

[39] Ghosh SK, Functional Coatings by Polymer Microencapsulation. 2006 WILEYVCH Verlag GmbH & Co. KGaA, Weinheim.
[40] Bakul DC, Bruce D, Joan VS, Jeffrey ZI, Sol-gel encapsulation methods for biosensors. Analytical chem. 66 (1994) 1120A–1127A.
[41] Bush JA, Beyer R, Trautman R, Barbé C, Bartlett C, Ceramic Micro-Particles Synthesised using Emulsion and Sol–Gel Technology: An Investigation into the controlled release of encapsulants and the tailoring of micro-particle size. J. Sol-Gel Sci. Techn. 32 (2004) 85–90.
[42] André V, Lydie V, Sabrina V, Jean LB, Use of ionic liquids in sol-gel; ionogels and applications, CRAS2C-3171; pp.14.
[43] Li ZH, Zhen J, Luan JY, Mu TC, Ionic liquids for synthesis of inorganic nanomaterials, Current Op. Solid State Mat. Sci. 12 (2008) 1–8.
[44] Chou K-S, Chen C-C, Fabrication and characterization of silver core and porous silica shell nanocomposite particles, Micropor. Mesopor. Mat. 98 (2007) 208-213.
[45] Zhang Q, Zhang TR, Ge JP, Yin YD, Permeable Silica Shell through Surface-Protected Etching, Nano Lett. 8 (2008) 2867-2871.
[46] Liu B, Xie WX, Wang DP, Huang WH, Yu MJ, Yao AH, Preparation and characterization of magnetic luminescent nanocomposite particles, Mat. Lett. 62 (2008) 3014–3017.
[47] Pucher P, Azouani R, Kanaev A, Krammer G, A Photocatalytic Active Adsorbent for Gas Cleaning in a Fixed Bed Reactor, Int. J. Photoenergy (2008) 759736.
[48] Brinker CJ, Scherer GW, Sol-gel Science: the physics and chemistry of sol-gel processing, San Diego CA, 1990, Academic Press Inc., 908 s.
[49] Maruszewski K., Strek W., Jasiorski M., Ucyk A., Technology and Applications of Sol-Gel Materials, Rad Eff Def Sol 158 (2003) 439-450.
[50] Tjong S.C., Chen H., Nanocrystalline materials and coatings, Mat. Sci. Eng. R 45 (2004) 1-88.
[51] Hughes A., Nanostructure-mediated drug delivery, Nanomed.: Nanotechn., Biol. Med. 1 (2005) 22-30.
[52] Borak B., Laskowski S., Heczko O., Aaltonen A., Baszczuk A., Jasiorski M., Söderberg O., Mazurek B., Oja M., Hannula S-P., Maruszewski K., Synthesis and properties of sol-gel submicron silica powders doped with iron crystallites, J. Sol-Gel Sci.Techn. 41 (2007) 185-190.
[53] N. Mahmed, O. Heczko, O. Söderberg, S-.P. Hannula, Room Temperature Synthesis of Magnetite (Fe3-δO4) Nanoparticles by a Simple Reverse Co-Precipitation Method, 3rd Int. Congr. Ceramics (ICC3) Nov 14-18, 2010. "IOP Conference Series: Materials Science and Engineering"

Functional polymer and hybrid capsules

Core-shell structured polymers like multibranched block copolymers, dendrimers and hyperbranched polymers may be used as carriers for various low molar mass substances. By selecting suitable core shell combinations and suitable functional groups it is possible to make the microcapsules stable at either acid or base environments and release the active components as the surface properties change. The permeability is affected by the polymer structure, molecular weight and polymer/activates concentrations and solubility properties. The size of the capsules should be controlled since large particles affect the coating matrix integrity.

Ideally, dendrimers constitute a class of well-defined, “perfectly” branched, globular macromolecules, typically 1-10 nm in size. Dendrimers are produced in an iterative sequence of reaction steps; each additional iteration leads to a higher generation material that carry a multiplicity of functional groups at their periphery. This stepwise synthetic procedure enables precise control of the architecture and surface functionalities, and makes it possible to tailor the physical and chemical properties [54,55]. Due to the demanding synthesis the dendrimers in general are expensive [56] and their potential applications are in high added values e.g. biomedical applications, [57,58] though they are excellent reference materials for encapsulation. Hyperbranched polymers offer the adjustable properties similar to perfectly globular dendrimers (materials in the same class), and their easy synthesization makes them more attractive for researchers and manufacturers. Therefore, they are ideal candidates for replacing dendrimers when less structural perfection is required. Even though with these materials novel development opportunities are available, they are not yet used much as bioactive carriers, in composite materials and nanocarriers. Also, organic bowl shape cavities can be used for capsulation. In organic solvents, the majority of these synthetic supramolecular assemblies rely on H-bonding and metal coordination. Most of these containers, such as calixarenes, resorcinarenes and cyclodextrins, are constructed using only covalent bonding providing a long residency times and means to isolate guests that normally have only a brief existence. Also, the binding are dependent on media and guests how complexes are formed. In addition, amphiphilic polymers can be exploited to achieve microcapsules which are environmentally sensitive for external stimuli, such as pH and temperature.

[54] Newkome G.R., Moorefield C.N., Vögtle F. Dendrimers and Dendrons, Wiley-VCH, Weinheim, 2001.
[55] Dendrimers and Other Dendritic Polymers, Fréchet JMJ, Tomalia DA (eds) Wiley-VCH, Weinheim, 2001.
[56] Chem. Eng. News 83 (2005) 30-36
[57] Helms B, Meijer EW, Science 313 (2006) 929.
[58] Stiriba SE, Frey H, Haag R, Angew. Chem. Int. Ed. 2002, 41, 1329.

4. Methods and materials

4.1 Synthesis and characterisation of polystyrene (PS) based microcapsules

A simple preparative laboratory procedure for the encapsulation of 3-Iodo-2-propynyl N-butylcarbamate (IPBC) into PS-based microcapsules was developed. The composition of the PS capsules was modified by using PCL, PAA and PBA polymers. The PCL was added to the composition to tailor the hydrophobicity of the capsules and hence the release profile of IPBC into water. PAA was used in order to introduce pH-responsive behaviour and respectively PBA was used to modify the mechanical properties of the PS. We used a simple oil-in-water (o/w) *emulsion solvent evaporation technique* in the production of microcapsules from common dichloromethane (DCM) solvent. Emulsion solvent evaporation method utilizing dispersed organic phase and an aqueous continuous phase (o/w emulsion) was applied in the production of the PS-based microcapsules. One liter volume D100 mm round bottomed glass reactor equipped with Heidolph RZR 2052 overhead stirrer and a 80 mm VISCO JET® impeller (VISCO JET Rührsysteme GmbH) was applied. The top of the reactor was open to allow evaporation of the organic solvent.

Microscopy characterization

Scanning electron microscopy with microanalysis (SEM-EDS) was utilized in determining the distribution of iodine in the microcapsules. In addition, the *Atomic force microscopy* (AFM) was used to analyse the cross-cut sections prepared for SEM-EDS analysis. The AFM analysis was performed using AFM phase imaging (Park Systems XE-100, hard tapping, Nanosensors ACTA silicon cantilevers) to reveal the microstructure of the PS/PCL within the microcapsules. *Polarized light Optical microscopy* was utilized to study the phase separation of the PS and PCL polymers cast on microscope glass slides. 50 µl of the 2 wt-% polymer solution (1 mg of polymer) in DCM was pipetted onto the glass and the solvent was allowed to evaporate to the ambient air. The amount of polymer cast on glass corresponded to approximately 10 µm solid film thickness.

Chromatography measurements

High performance liquid chromatography (HPLC) was used to determine the IPBC concentrations in the microcapsules. The HPLC analyses were performed on a Shimadzu Prominence HPLC system consisting of two LC-20AD pumps, a SPD-M20A diode-array detector and a DGU-20A3 degasser. The samples were chromatographed on a Phenomenex Gemini NX, 250 x 4.6 mm C18 reversed phase column. The eluent consisted of 65% acetonitrile in water. The flow rate was 1 mL/min. The IPBC concentration in the samples was quantified at 200 nm using a 7-point calibration curve of IPBC in the range 1–100 ug/mL (R^2>0.99). An exact amount of microspheres (7–8 mg) were dissolved in tetrahydrofuran (3 mL) by vortex mixing. An aliquot of the solution (50 µL) was then added to a solution of 70% methanol in water (950 µL) and mixed by vortex for 3 min and the mixture was filtered through a 0.45 µm PVDF membrane syringe filter before HPLC analysis. The samples were prepared in duplicates.

Release of IPBC from microspheres to water was studied using HPLC. To microspheres (*ca*. 17–19 mg) were added water (14 mL) and the mixtures were vortex mixed for 0.5 min and placed in the dark. The release of IPBC from the polymer microspheres into water was determined at time points 1–92 days by HPLC. The samples were prepared in triplicates.

The IPBC content of paint matrices was determined by HPLC analyses. First the IPBC content of the paint matrices were determined by weighing an exact amount (ca. 150 mg) of the paint matrice and adding acetonitrile (3 mL). The samples were vortex mixed for 1 min and then placed in an ultrasonic bath for 30 min. Before HPLC analysis, aliquots of 0.2 mL of the samples were diluted with 70% MeOH in water (0.8 mL), vortex mixed for 3 min and filtered. The glass wafers coated with different paint matrices were incubated in water (40

mL) in the dark. The amount of released IPBC was determined by HPLC. The samples were prepared in triplicates.

4.2 Synthesis and characterisation of silica based capsules

Two methods have been employed to synthesize silica particles: (i) Stöber method for dense silica particles; and (ii) water-in-oil mediated sol-gel method for hollow silica particles. Following chemicals were used in Stöber process to produce dense silica particles: ethanol was used as a solvent/reagent (Etax A, Altia, 96.1 vol%), deionized water (laboratory made) reacts with silica precursor to form silica particles, ammonium hydroxide (J.T. Baker, 24.5%) was used as a catalyst and Tetraethyl orthosilicate (TEOS, Acros Organics, 98%) was used as the silica precursor.

In Stöber synthesis the active agent i.e. the fire retardant material was inserted into the synthesis solution before addition of (TEOS) which was used as the silica precursor. Figure 2 shows typical composition of the modified Stöber method. The maximum particle size that is achievable by the Stöber method is around ~2 µm, while typical particle size achieved by the modified Stöber method was around ~1 µm. This creates a clear upper particle size limit which could be coated with Stöber method.

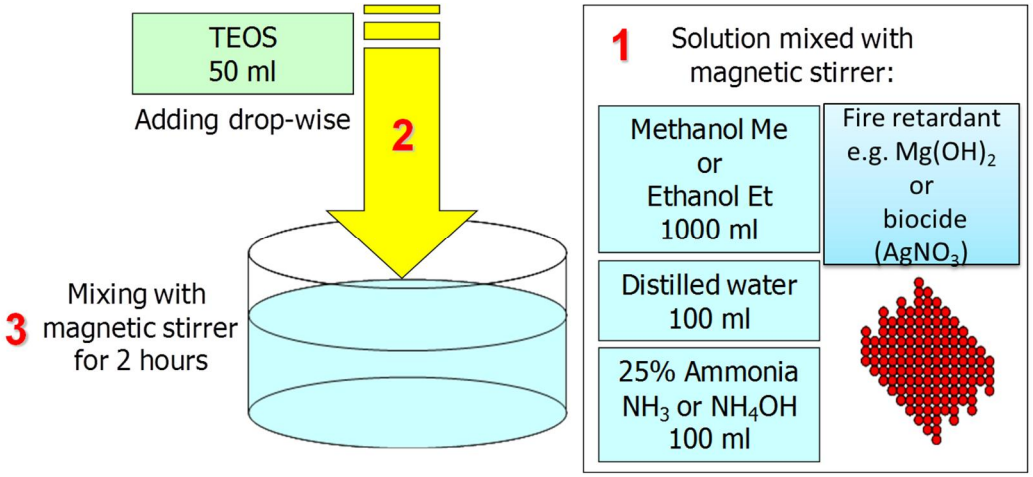

Figure 2. Modified Stöber method with fire retardant or biocide addition to the synthesis.

The hollow porous silica microspheres were synthesized by W/O emulsion combined with sol-gel technique, see Figure 3. First, the oil phase was prepared by dissolving 1.6 g HPC in 250 ml 1–octanol, the mixture was heated at 353 K and mixed by a magnetic stirrer with heating for 0.5 h. Then 6.2 ml of Span 80 was added to the oil phase, and was kept at 313 K for 0.5 h. Second, the water phase was prepared by mixing 2.2 ml ammonium hydroxide in 21 ml of deionized water by a magnetic stirrer for 0.5 h. Then 1.7 ml Tween 20 was added, and the mixture was stirred for another 0.5 h. Then the water phase was mixed into the oil phase at 313 K and mixed for 0.5 h and after that 64.5 ml of TEOS was added drop wise to the emulsion. The molar ratio of TEOS : water : ammonium hydroxide was kept at 1 : 4 : 0.2 and the solution was left to stir for 6–72 h. After this the powders were typically aged for 9–48 h in the solution without any stirring and then washed with ethanol repeatedly and centrifuges for 3 min. The resulting white particles were dried in air for 24 h, and finally calcinated in air at 773 K for 3 h.

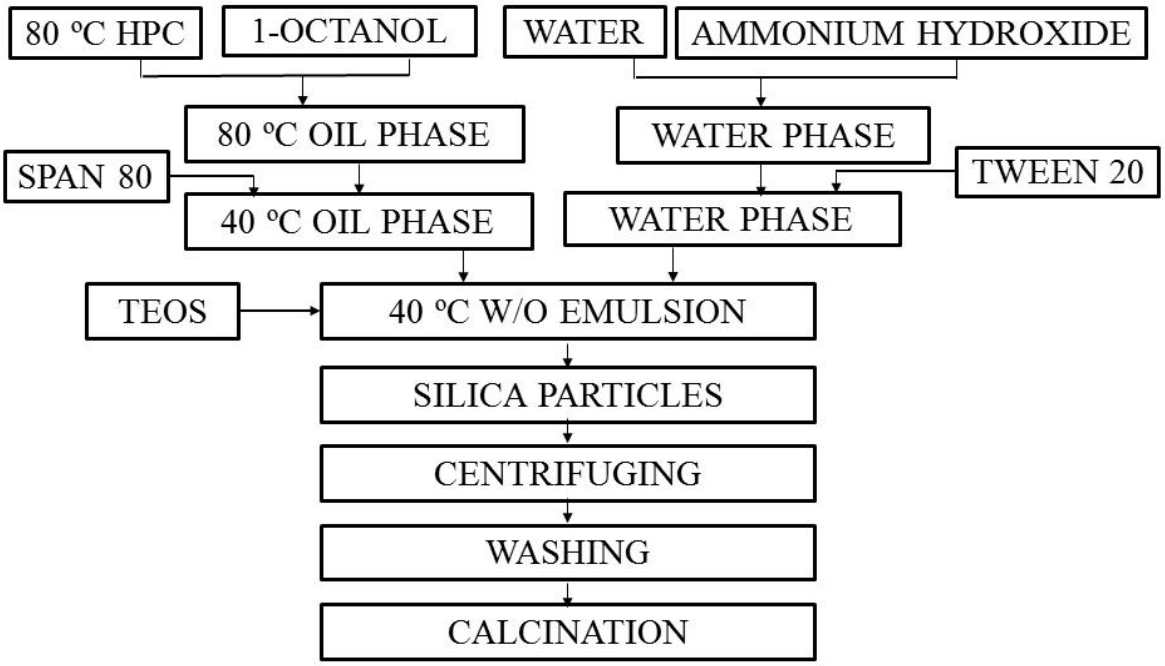

Figure 3. The process of W/O emulsion combined with sol-gel technique.

4.3 Particle emission experiments

The tests for particle emissions during abrasion of the paint boards were made to manage the potential environmental and safety concern of the coatings modified with microcapsules. Real-time instrumental monitoring reveals levels continuously during the abrading task as well as information about peak exposure, which is not available from filter-based procedures. Therefore, we made both real-time sampling in the close vicinity of the source of emission (abrasion instrument) and filter-based measurements to clarify changes in dust amounts, particle sizes, shape and content. As the distribution of inhalable, thoracic, respirables (alveolics) particles are too low for gravimetric measurements all real-time follow up was performed with electronic measuring devices.

The dust content and particles sizes were measured with five different ways (Figure 4). The simulation of emission of biocides, microcapsules and dust particles from painted wooden boards were made by using a washing and scrubbing resistance instrument (Erichsen Washability and Scrub Resistance Tester, Model 494 MC) to clarify the effects on the tread. The instrument was equipped with a sled (DIN 53 778) and a brush (DIN 53778/B4) which weight was 115 g. The abrasion pad was covered with sand paper with a different fineness of grind (Silicon carbide wet and dry 180 - 400 particle size). The 240 particle size paper was found the best for these experiments, because it did not block in the process and it seemed to strip the most paint from the surface.

The tests were made with four different types of painted pine boards (thickness 18 mm, length 450 mm, width 100 mm): pine boards painted with 1) acrylate paint (Ultra-Classic-A-pm G966001, Tikkurila, Finland, C0-1K), 2) biocide modified acrylate paint (C0-1K Model), 3) IPBC-Texanol (20:80 mixture) modified acrylate paint (C1-K1) and 4) PS-IBPC modified acrylate paint (C1-K5). The wood panels were painted 18 hours earlier and were dried 4 hours in 40 °C degrees.

Figure 4. The instrumentation for particle emissions during the abrasion tests.

Analysis of the particle emissions

Dust particles were also collected on a polycarbonate filter (pore size 0.8 µm, flow rate 6.23 l/min) and the inlet was approximately 25 cm from the moving sled. The collection time was 6.5 hours. Particle distribution and shapes and chemical content were measured by transmission electron microscopy (TEM) equipped with energy dispersive X-ray spectroscopy (EDS) and the elemental line scans were made showing the elemental distribution on a sample surface.

In the continuous measurement in real time, particles were measured in 15 channels and the data was presented as the distribution of inhalable, thoracic, respirables (alveolics) particles (15 Channel Real Time Aerosol Spectrometer Grimm model 1.108, a resolution of 1 count/liter, channels from 0.30 µm to 20 µm, scanning time was 6 sec). A random sampling head collects the dust in accordance to the Johannesburger Convention and leads the particles directly into the optical chamber with the laser. There each particle is counted and classified by size and the concentration is proportional to the collected time.

Particle mobility size distributions were measured in 13 channels from 10 to 365 nm with an aerosol mobility spectrometer (NanoScan, TSI Model 3910, sample flow rate 0.75 L min^{-1}, cyclone at inlet with a cut-size of approximately 500 nm, scanning time was 45 sec with 15 sec retrace). Sampling line was 30 cm conductive rubber tube which diffusion losses were corrected according to Cheng (Cheng, 2001). Sample inlet was approximately 20 cm over the abrasion table.

Particle size distributions were optically measured in 16 channels from 335 nm to 8.96 µm with an optical particle sizer (OPS, TSI model 3330, sample flow rate 0.97 L min^{-1}). Sampling line was a 30 cm long conductive rubber tube. During the first experiment, sampling time was

1 min after which it was changed to 15 sec because duration of the abrasion process was only some minutes. The sample inlet was approximately 20 cm over the abrasion table.

Total particle number concentration was measured with a condensation particle counter (CPC, TSI Model 3007, sample flow rate 0.9 L min^{-1}). The sample inlet was approximately 40 cm sideward of the abrasion table. Numerical particle size distributions were converted to mass distributions by assuming spherical particles with unit density (1 g/cm^3). In conversion, particles mobility diameter and optical diameter were assumed to be equivalent.

5. Results

5.1 Polymer based microcapsules for anti-fouling paints

The following Table 4 presents the studied sample compositions, mean particle sizes and encapsulation efficiencies.

Table 4. Samples for the IPBC release testing.

	Composition (w/w-%)	**Mean particle radius *r* (µm)**	**IPBC in the microspheres (%)**	**Encapsulation efficiency of IPBC (%)**
PS-PCL-1*	100/0	12	10.6	71
PS-PCL-2*	75/25	13	6.6	44
PS-PCL-3*	50/50	12	6.4	43
PS-PCL-4*	25/75	12	6.0	40
PS-PCL-5*	0/100	12	5.7	38

*) the encapsulated fraction of the 15.0 wt-% of IPBC in the feed. M_w(PS)=283 kDa (SLS in toluene), M_w(PCL)=14 kDa (Sigma-Aldrich)

AFM imaging

Figure 5 presents AFM topography and Phase images of PS/PCL microcapsules. IPBC particles appeared in the AFM topography images as slightly bright <1 µm spots sparsely distributed on the surface. Only the particles directly exposed to the surface were visible. The IPBC can be also resolved from the phase images as slightly brighter areas, especially in the PCL rich samples (D and E). The IPBC was predominantly located in the more hydrophobic PS rich phase. In the blend compositions PS rich (A and B) the IPBC was found better dispersed and more coherently wetted by the matrix polymer than in the PCL rich compositions (D and E). Phase signals suggest fine, phase separated and co-continuous morphologies for all compositions containing PCL. The brighter areas of PCL dendritic particularly well presented in the PS-PCL 75/25 composition (B). It is noteworthy that the studied surfaces samples prepared by mechanical polishing and hence subject to sample preparation artifacts, which were visible in the images as nanoscopic scratches (in -30° to -60° angles).

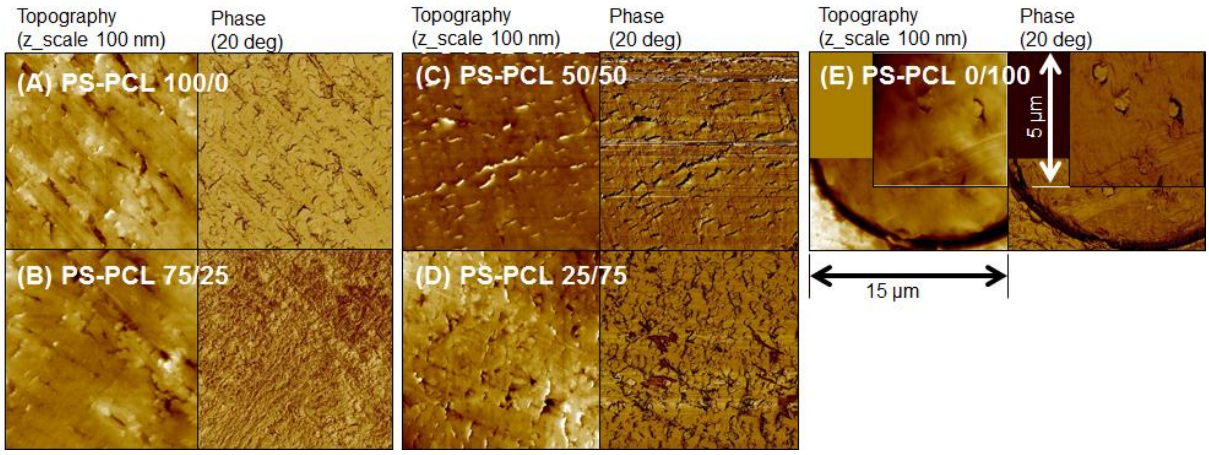

Figure 5. AFM topography and Phase images of PS/PCL microcapsules containing IPBC. Scan size 15 µm, inset images 5 µm. Z-range 100 nm. (Re-prints with permission from Journal of Microencapsulation)

Optical microscopy

Figure 6 presents polarized light optical images of PS-PCL solvent cast films of eleven compositions 100% to 0% PS. Different compositions are indicated by letters A-K, respectively. The 100/0 PS-PCL (A) appeared totally amorphous and hence transparent. The composition 0/100 PS-PCL (K) presented a fine crystalline morphology consisting of PCL. In all other compositions (B-J) the film consist of a PS rich and PCL rich phases formed by spinodal decomposition, as previously reported for PS/PCL blends utilizing different solvents and matching molecular weights (both high/low) for the PS- and PCL components. In the equilibriated (annealed) films the PS rich phase was layered on top of the PCL rich film covering the glass substrate, as clearly evidenced by (D-G). At composition PS-PCL 90/10 (B) the morphology presents a very fine continuous network of PCL dendritic crystals embedded in the PS matrix. At range of compositions 30/70 to 10/80 (H-J) the PS rich phase form rounded non-connected area, indicated by purple color.

Hence, according to the optical images the low molecular weight PCL has appreciable solubility in high molecular weight PS the composition PS/PCL 90/10. The resulting phase separated morphology has significantly finer and more interconnected features than the other blend compositions.

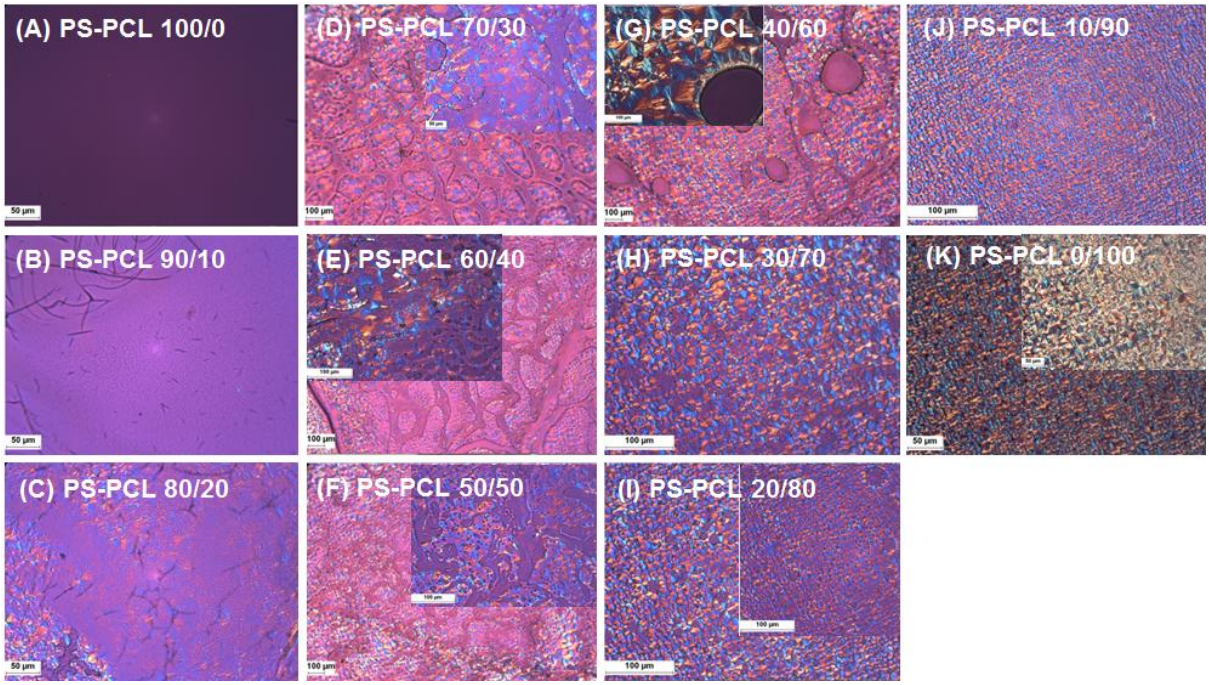

Figure 6. Polarized light optical images of approximately 10 µm PS-PCL cast films on microscope glass slide. The blend composition of the films was varied from pure PS (A) to pure PCL (K). (Re-prints with permission from Journal of Microencapsulation)

SEM

PS-IPBC capsules were studied with SEM by applying a -100 V to the secondary electron detector. Thus the SE electrons with energy less than 50 eV were excluded and the contrast was coming from atomic weight differences like in back scatter mode. Particles were mounted into epoxy and ground before SEM imaging, no coating was applied. Figure 7 (a) is from RC2 which contains 37.5 wt.% of IPBC and the (b) is from RC3 which contains 7.5 wt.% of IPBC. The RC2 contains visibly more light gray areas (IPBC) than RC3.

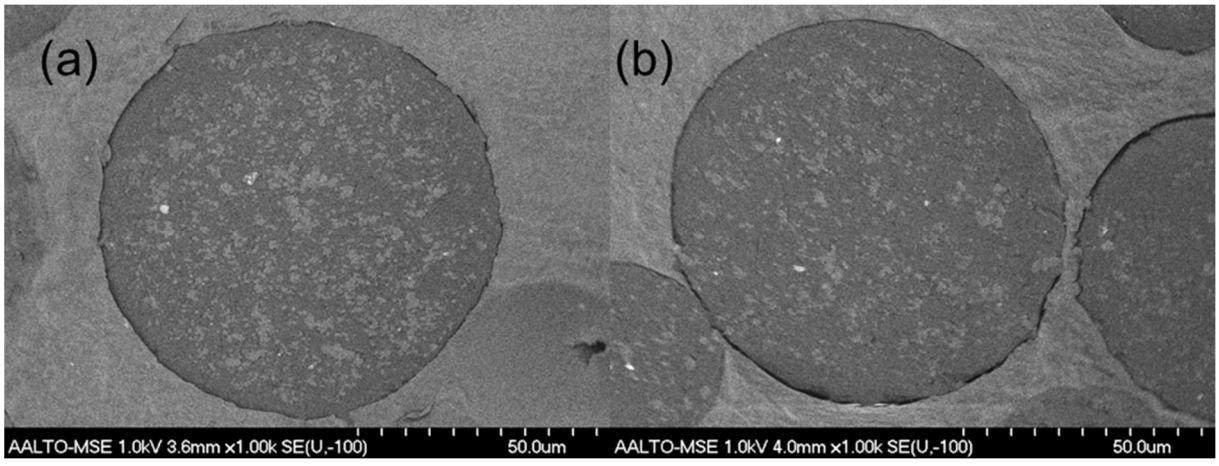

Figure 7. (a) Energy filtered SEM images of RC2 containing 37.5 wt.% IPBC and (b) RC3 containing 7.5 wt.% of IPBC. The white/light gray particles are areas rich in Iodine (IPBC).

All powders were mounted in epoxy and ground to produce cross section samples. Pure polystyrene sample contained highest amount of light gray areas which should be the case since according to HPLC analysis it contained highest amount of IPBC (10.6%), when the amount of polycaprolatone was increased (sample PS-PLC 2 and PS-PLC 3) in the powders the less IPBC rich areas could be detected as seen in Figure 8 (a-c). In PS-PLC4 the IPBC rich areas were a bit more common than in PS-PLC3 as seen in Figure 8 (c) and Figure 9 (a). However, the PS_PLC5 sample which was made fully of polycaprolactone seemed to have almost no IPBC rich areas on the particles, Figure 9(b).

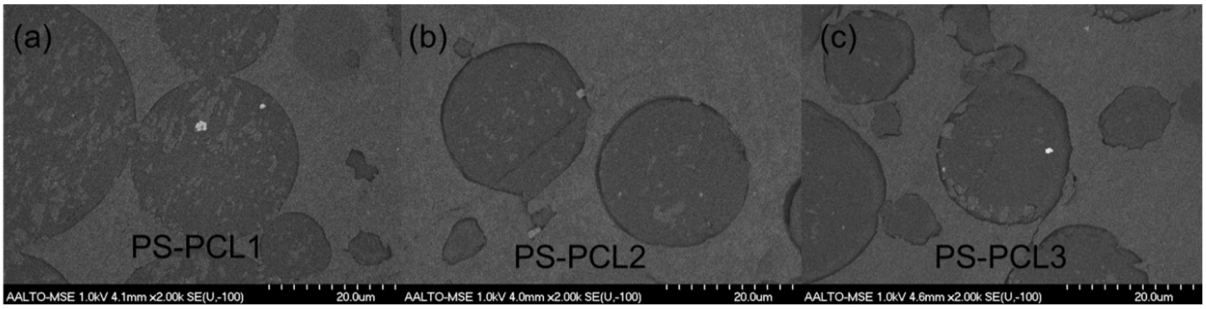

Figure 8. Energy filtered SEM images of cross sectioned samples of: (a) PS-PLC1, (b) PS-PLC2 and (c) PS-PLC3. As the amount of PLC was increased the less IPBC rich areas could be seen.

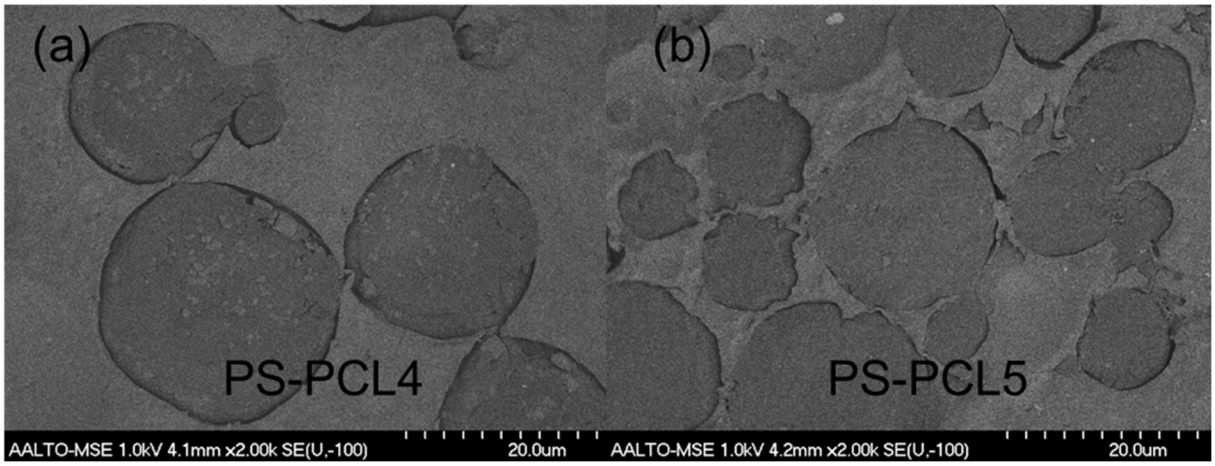

Figure 9. Energy filtered SEM images of cross sectioned samples of: (a) PS-PLC4 and (b) PS-PLC5. As the amount of PLC was increased the less IPBC rich areas could be seen.

NMR

All PS-PCL samples were analysed by ^{1}H NMR spectrometry. About 30 mg of each sample was dissolved in deuterochloroform and the ^{1}H NMR spectra were recorded. In all samples the signals from IPBC were detected (Figure 10).

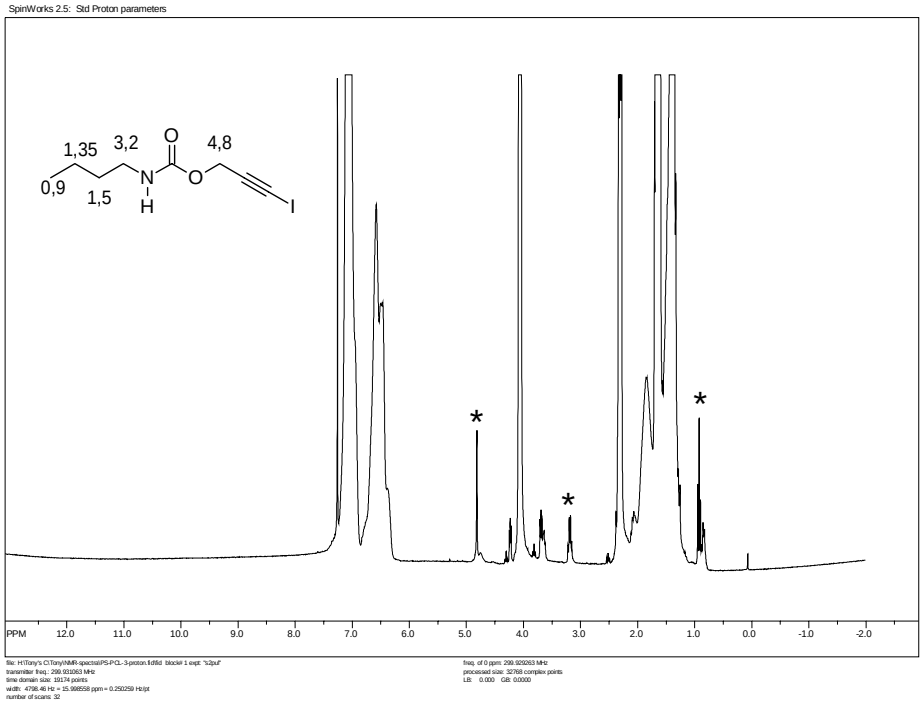

*Figure 10. 300 MHz ^{1}H NMR spectrum of sample PS-PCL 50/50 in $CDCl_3$. Protons from IPBC are marked in the figure as *.*

Release of IPBC from microcapsules

Figure 11 presents the release data for the PS-PCL blend compositions (1–5). For all the compositions an initial burst of IPBC release was observed. The released mass fraction in the initial burst was consistently higher for the compositions containing PCL, which is in line with the increased hydrophilicity of the microspheres. After the initial burst the release rates are decreasing to µg/d range, which is significantly less than reported for IPBC release in the previous studies. In an appropriate water permeable matrix material, such low rate from the PS-PCL microcapsules would enable sustained release of IPBC at least several months past the 92d time point. It is noteworthy that the presented data is the accumulated release without changing the water between the time points. The released mass of IPBC in water is still well below the saturation concentration (approximately 150 mg/L at RT).

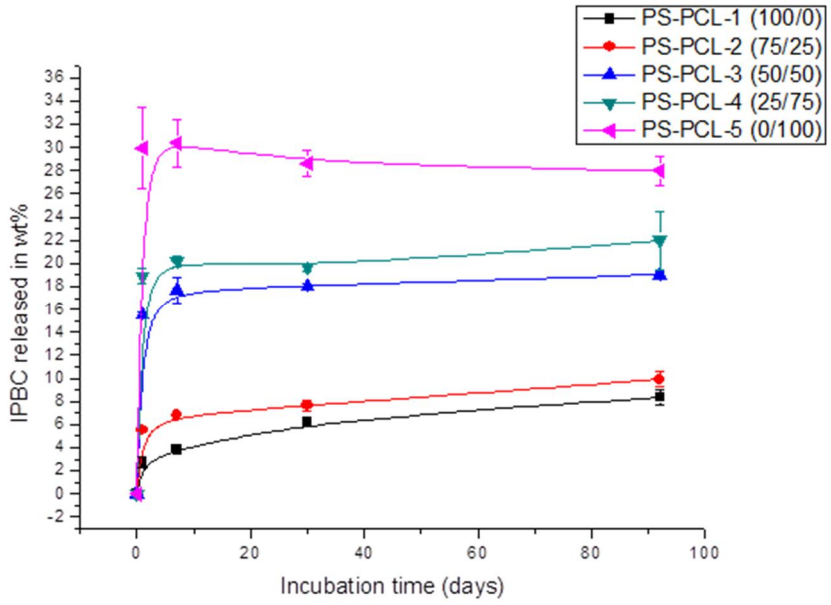

Figure 11. Accumulated released mass fraction of the IPBC from the PS-PCL microspheres at time points 1d, 7d, 30d and 92d.

5.2 Anti-fouling properties of biocide-modified paints and varnishes

The IPBC content of different wet paint matrices and the release of IPBC to water were determined by HPLC analyses. The IPBC content ranged from 0.9–1.1 wt% and the amount of IPBC released to water was determined during a 1 month period for the paint matrices (Figure 12).

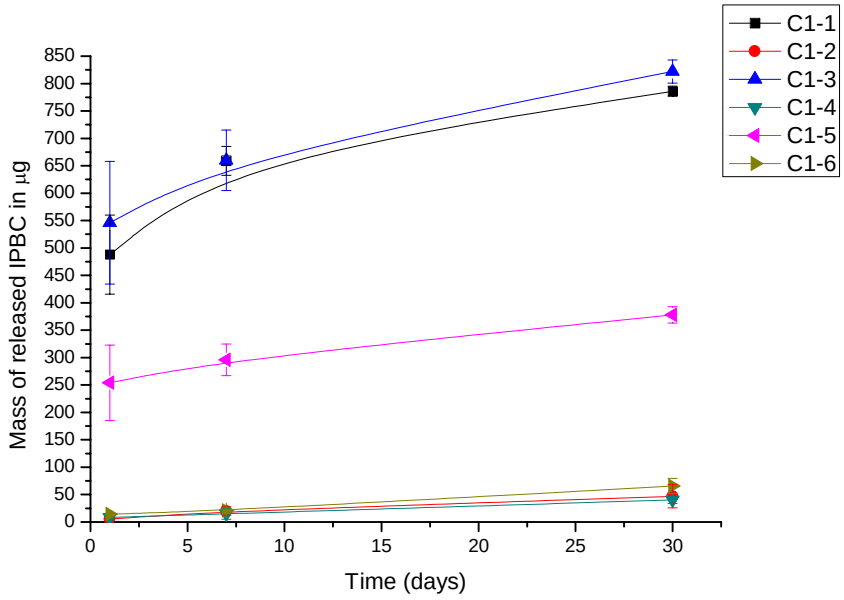

Figure 12. Release of IPBC to water from paint matrices on glass wafers.

The mould growth of the coatings on glass plates after 20 weeks incubation time was reported in the previous report. The results after 40 weeks incubation time are presented in Figure 13 and Figure 14. The surface of the reference birch veneer was fully covered with the mould after six weeks of exposure (Figure 13 and Figure 14). The mould growth on glass surfaces coated with polyurethane lacquer or paint was slow (Figure 13 and Figure 14). After changing the new agar substrate after 18 weeks the mould index increased slowly from 2.5 to 3 with sample having no fungicide in lacquer. Some increase in mould index was also found in sample containing commercial encapsulated fungicide (mould index from 0 to 1). With the other lacquer samples no increase in mould index was found. During 40 weeks of incubation no growth was seen on the surfaces of lacquers containing commercial encapsulated IPBC (Fungitrol) which was leached with water before the test. In addition the mould growth was very small (mould index is 1) with the other IPBC containing samples.

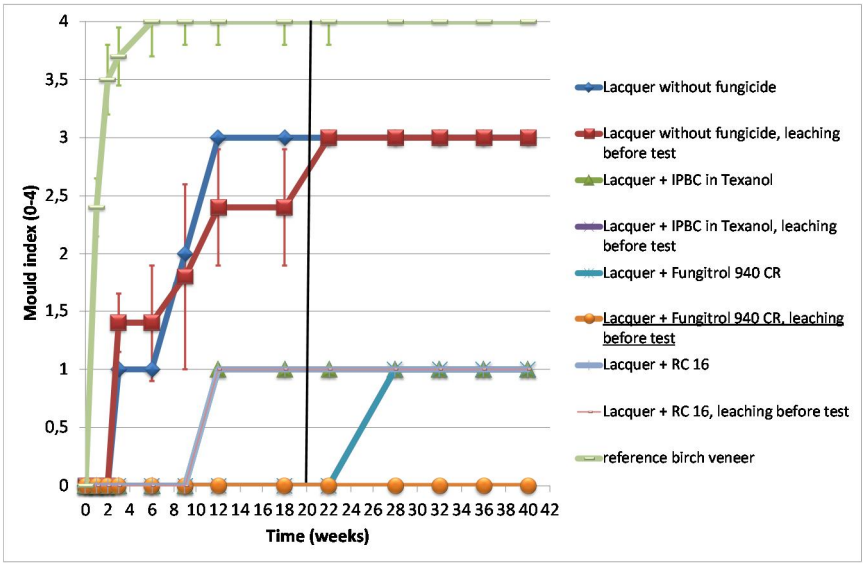

Figure 13. Effect of biocide to moulding of 2-component polyurethane lacquer.

The mould growth on paint surfaces was even slower and smaller than on lacquer surfaces (Figure 14). Mould growth of the paint samples containing no fungicide reached the level 2 – 3. After 40 weeks of incubation no growth was seen on the surfaces of paints containing IPBC suspended in Texanol or containing synthetized RC-capsules Like with the lacquer samples the mould growth was very small (mould index is 1) with the other IPBC containing samples.

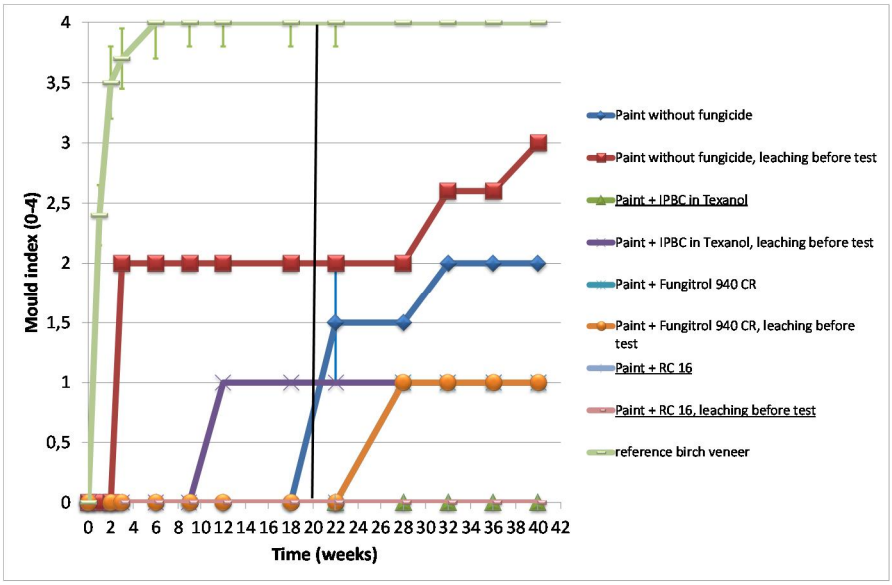

Figure 14. Effect of biocide to moulding of water based paint.

5.3 Emission studies of capsule-loaded coatings

The microcapsules used in our project were round and oval in shape. We are all being made increasingly aware of the potential impact our activities may have on the environment as well as for workers during painting and sanding surfaces. The paints can affect the balance of aquatic life as well as health of humans. We concentrated our study to down-stream applications e.g. manipulating and machining of painted boards containing microcapsules produced in this project and comparison of them to commercial paints where the biocide was added by the manufacture as well as to pure paint and lacquered surfaces. As the paints were done in laboratory scale we could not study the exposure with the workers in rebuilding or recycling even though workers are generally exposed to higher levels than the general population.

The dust's distribution on inhalable, thoracic, respirables (alveolics) particles was collected during the abrasion of the paint surfaces. The amount of the dust was very low and also the moving around the instruments seemed to produce as much dust as the abrasion procedure itself. In Figure 15, the changes during the abrasion of the four different paints are presented. The measured background amount of dust was 2.0 mg/m^3 or below for all fractions.

Large amount of titanium was found in the particles. The large copper peaks are coming from the holders of the instrument. The largest particles are from ripped paint. The EDS scan and the shape of the particle are presented in Figure 16. Most of the particles were diesel type and sulfur-containing particles (particle size less than 1 µm), dander particles, and slightly larger about 4-30 µm titanium containing particles.

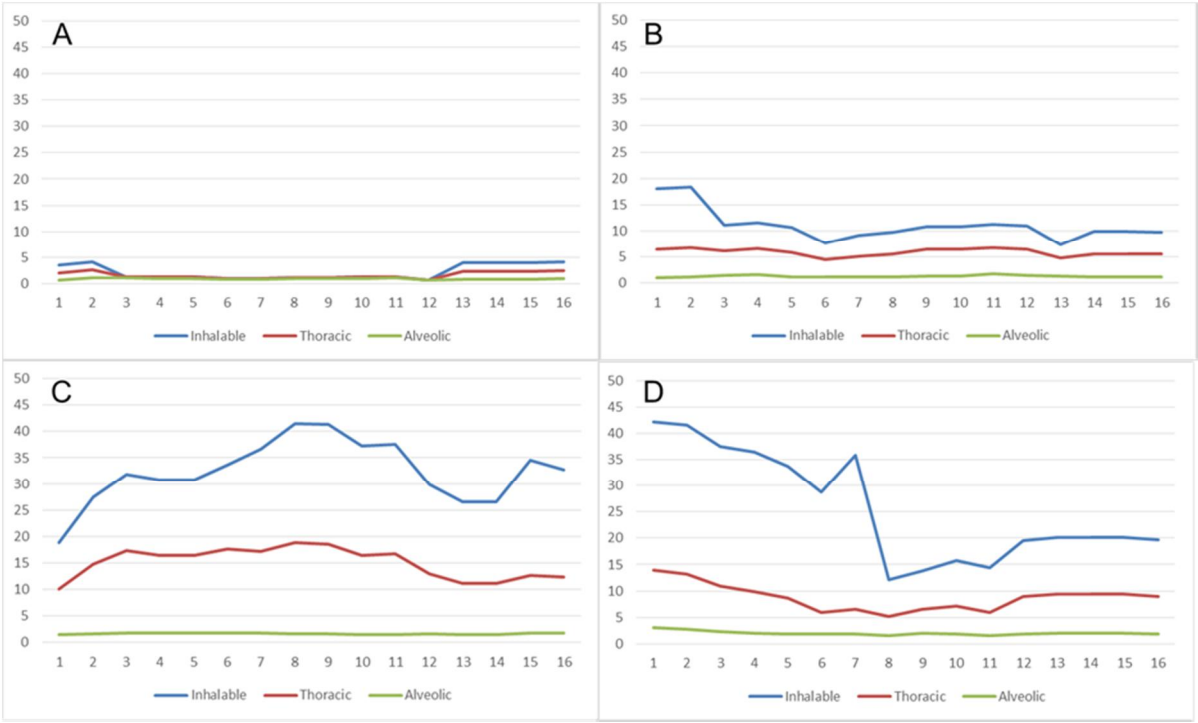

Figure 15. The dust distribution on inhalable, thoracic, respirables (alveolics) particles. 50 abrasion cycles, wet and dry sand paper SiC2 particle size 240. A) Pure paint, b) Paint + manufacture added biocide, c) Paint + IPBC-Texanol (20:80), d) Paint + PS-IPBC.

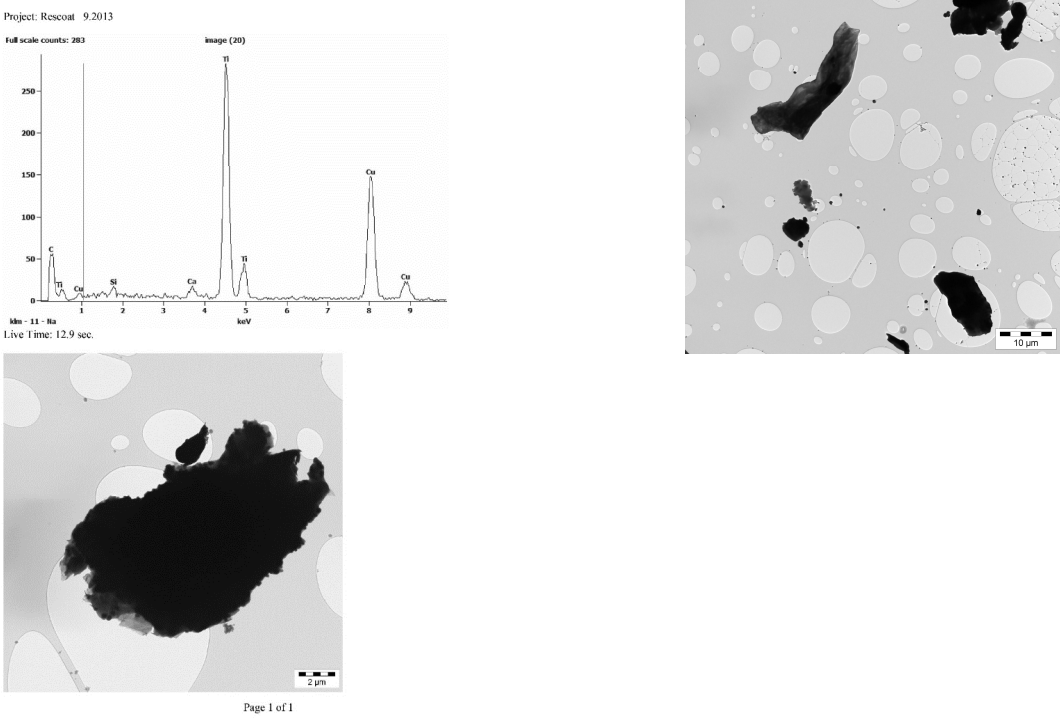

Figure 16. Paint particle and its ESD scan on left. General overall figure from the dust on right.

5.4 Microcapsules for self-healing polyester paint

Polystyrene (PS) microcapsules were prepared and used for encapsulation of isophrone di-isocyanate (IPDI) to create self-healing performance. The IPDI is known for its self-polymerisation after initiated by moisture. Therefore, the reactivity of IPDI was hindered by blocking the reactive isocynate groups (-N=C=O) using 2-butanone oxime. The blocking reaction is described in Figure 17.

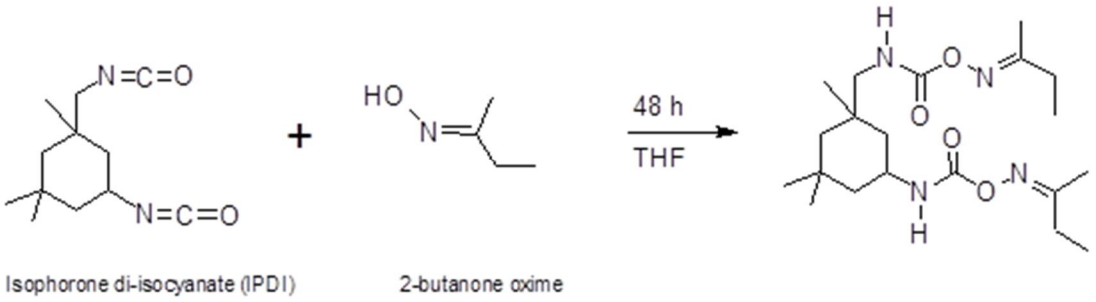

Figure 17. End-blocking of isocyanate groups for hindered reactivity of IPDI.

PS microcapsules with IPDI self-healing agent were similarly prepared as described in chapter 3.2. In step 1, PS-DCM solution was prepared by dissolving 2 wt% PS polymer into dichloromethane (DCM) solvent. In step 2, the blocked IPDI was added with different loadings into PS-DCM solution. In these experiments blocked-IPDI loading was 15 wt% (RC 33) and 40 wt.% (RC 34) of polystyrene amount, respectively. In step 3, PS-IPDI solution was added dropwise into 2 wt% aqueous PVA solution while stirring vigorously. Finally, in step 4 the reaction solution was mixed until DCM was fully evaporated.

The self-healing coatings were prepared by mixing 10 wt% and 17.4 wt% of the PS-IPDI microcapsules into polyester paint (provided by Ruukki). In order to remain the microcapsules free of cracks, a gentle mixing of the microcapsules was done by using glass tube (Figure 18a). The solutions were brushed on metal sheets and cured using thermal treatment at 150 ^{o}C (Figure 18b).

Figure 18. (a) PS-IPDI microcapsules mixed into polyester paint and (b) Polyester paints with and without PS-IPDI microcapsules.

Scanning vibrating electrode technique (SVET) measurements were conducted in order to study the self-healing performance of coatings. Performance of polyester paint was studied with and without microcapsules. Figure 19 presents the comparison of SVET results for reference polyester paint and PS-IPDI-modified polyester paint. The point defect made to the coating with a needle was detected by the scanner. The ionic currents (μA/cm^2) in 0.005 M NaCl solution were detected for both reference and polyester paint with 17.4 % PS-IPDI capsules. Apparently, the painted surface with PS-IPDI microcapsules showed lower ionic currents during the measurement time.

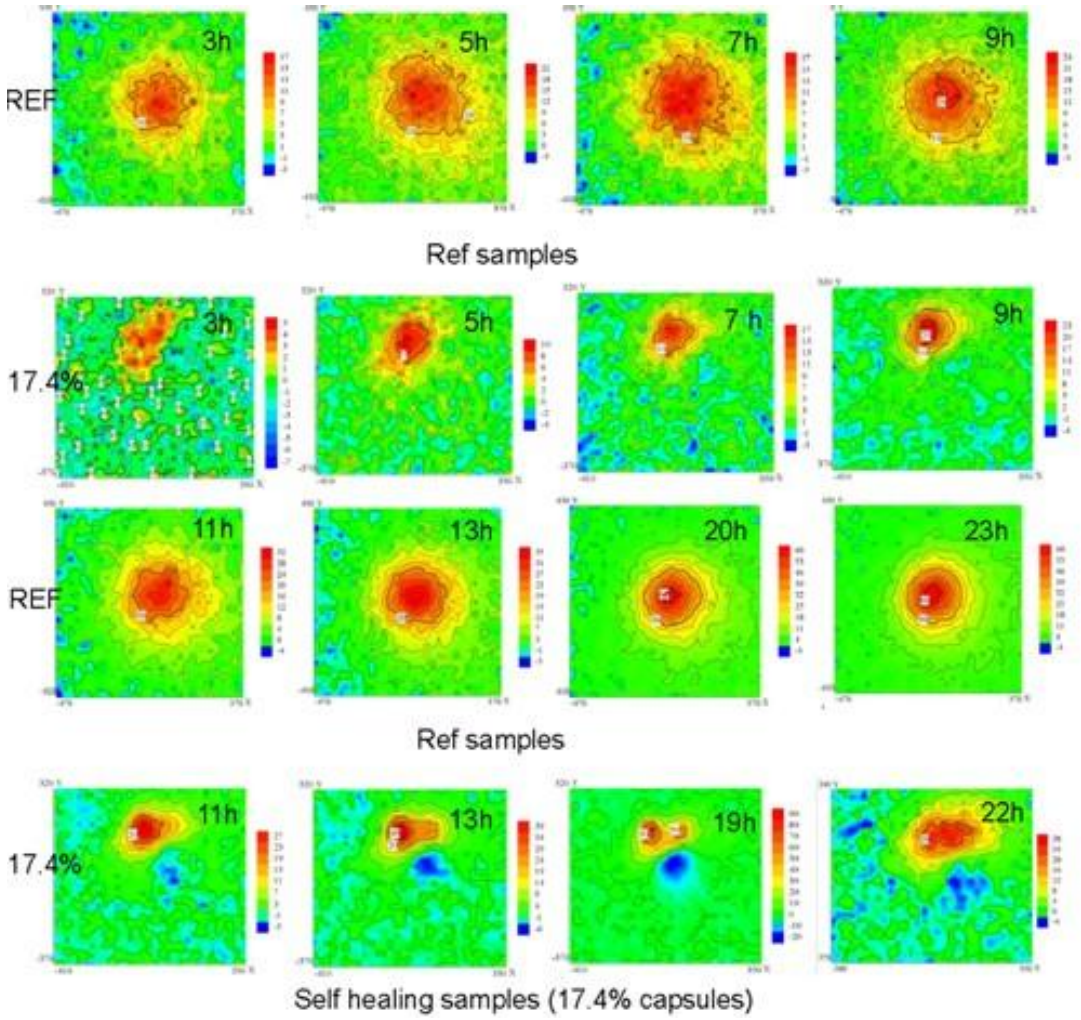

Figure 19. a) SVET comparison (ref polyester paint vs PS-IPDI-17.4% capsules).

Sample containing 17.4 % of PS-IPDI capsules for self-healing and reference sample of pure paint were also studied with localized electrochemical impedance spectroscopy (LEIS). The scratches were made on the paint layer exposing the bare metal. Samples were measured in 0.005 M NaCl solution with 8 lines each having 32 points. A new scan was made with 1 h intervals for 24 h to study the evolution of the measured system. The comparison between the reference pure paint and sample containing 17.4 % of capsules for self-healing is shown in Figure 20. The results showed lower values for the samples containing PS-IPDI microcapsules during the measurement time, indicating self-healing phenomena.

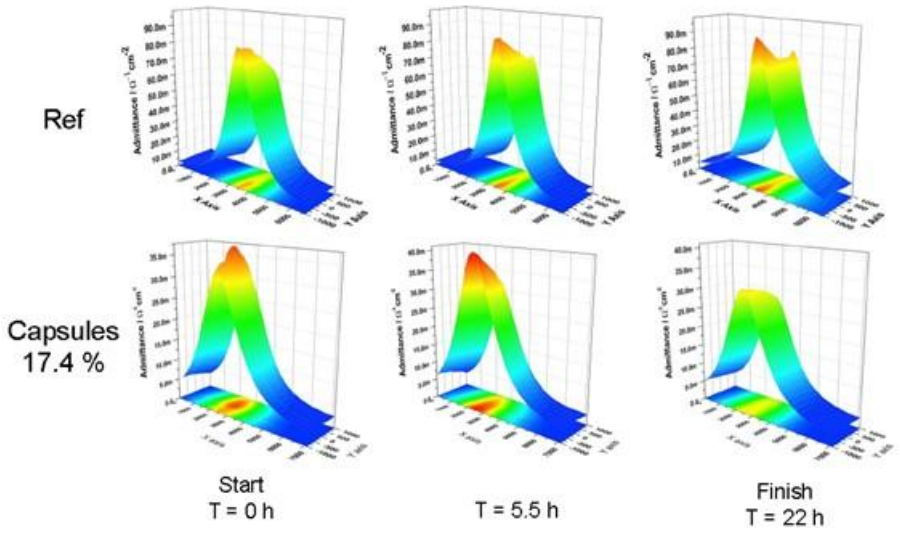

Figure 20. LEIS comparison for reference and sample containing 17.4% self-healing capsules.

5.5 Encapsulated antifreeze agent for anti-ice coatings

Hydrophilic and hydrophobic polymer matrixes were used for encapsulation of lithium salt (Li-salt) antifreeze agent. The hydrophilic polymer matrix was polyvinyl butyral (PVB) and respectively, the hydrophobic was polyvinylidene fluoride (PVDF). Polyethylene glycol (PEG) was blended with PVB to further enhance the hydrophilic character.

After mixing the solutions were cast on aluminium plates for the ice adhesion measurement. Figure 21 shows an example of the ice adhesion test setup and VTT's test apparatus. The measurements were conducted at -10 ^{o}C.

Figure 21. Ice adhesion test apparatus at VTT.

Table 5 summarises the measured ice adhesion values for different polymer matrixes and Li-salt contents. The lowest ice adhesion values were measured for PVB-PEG and PVDF. Indeed, the ice adhesion decreased by the increase of Li-salt content. The results indicated that PVB as such did not perform well as a host matrix for Li-salt.

Table 5. Effect of polymer matrix and Li-salt content on ice adhesion.

Polymer matrix	Li-salt [wt-%]	Ice Adhesion [MPa]
PVB	-	0.69 ± 0.04
PVB	3	0.33 ± 0.01
PVB	35	0.53 ± 0.03
PVB-PEG	0	0.58 ± 0.08
PVB-PEG	11	0.48 ± 0.03
PVB-PEG	23	0.50 ± 0.12
PVB-PEG	35	0.26 ± 0.11
PVDF	0	0.33 ± 0.09
PVDF	3.5	0.06*

*Only one sample measured

5.6 Silica based microcapsules

Further effort was made to optimize the water-in-oil (W/O) synthesis of hollow silica microcapsules. These results were combined to manuscript “The control of size and surface morphology of silica microspheres by Sol-Gel emulsion approach” (Chen, Friman, Vilonen and Hannula) which was accepted to be published in Suranaree Journal of Science and Technology. The emulsion system consists of water as internal phase, 1-octanol as external oil phase, multiple surfactants (HPS, Tween 20 and Span 80, and TEOS as silica precursor. The influence of solvent volume (80, 160 and 240 ml) and mixing speed (400, 800 and 1200 rpm) on the size and surface morphology of silica were investigated. Hollow particles were found in all samples, moreover, the structure also exhibits mesoporous feature, see Figure 22 and Figure 23.

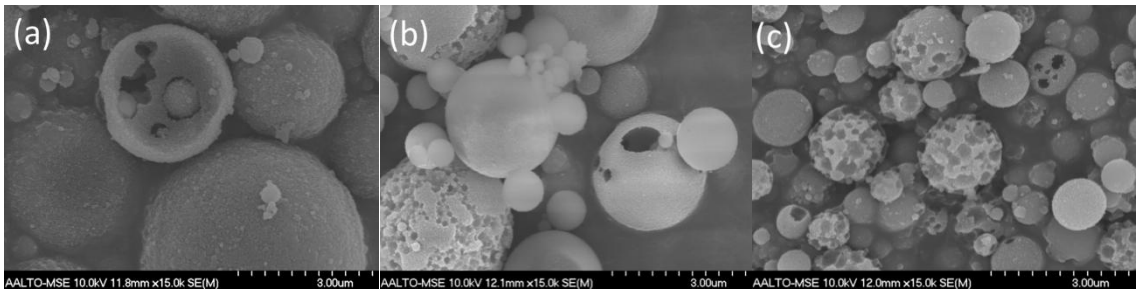

Figure 22. Electron micrographs of silica powders prepared by using different amount of 1-octanol: (a) 80 ml, (b) 160 ml, and (c) 240 ml.

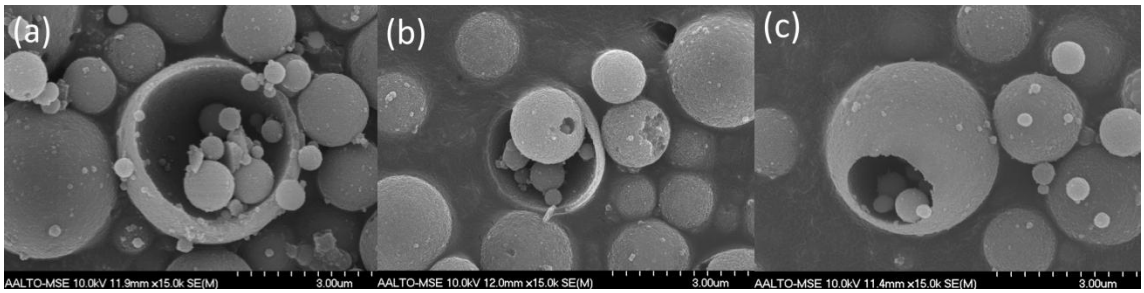

Figure 23. Electron micrographs of silica microspheres prepared by using different mixing speed: (a) 400 rpm, (b) 800 rpm, and (c) 1200 rpm.

The results reveal that particle size decreases as the solvent increased from 80 to 160 ml due to the decreased size of reverse micelles, and there was no significant difference in particle size when the solvent increased from 160 to 240 ml. Silica particles prepared by 160 ml 1-octanol also presents the greatest specific surface area and total pore volume. This meets our goal successfully on the process optimization in aspect of saving expensive 1-octanol.

Table 6. Properties of hollow silica microspheres prepared by different amount of 1-octanol.

Samples	**Volume of 1-octanol (ml)**	**Mean sphere size (μm)**	**Surface area (m^2/g)**	**Total pore volume * (cm^3/g)**
#1	80	4.8	140	0.277
#2	160	2.4	164	0.299
#3	240	2.8	115	0.193

*****above pore radius 1 nm

When the mixing speed was increased from 400 to 800 rpm, a clear decrease in particle size was observed (Table 7). When the mixing speed was further increased from 800 to 1200 rpm only a minor decrease in the particle size occurred.

Table 7. Properties of hollow silica microspheres prepared by using different mixing speeds.

Sample	**Mixing speed (rpm)**	**Mean sphere size (μm)**	**Surface area (m^2/g)**	**Total pore volume * (cm^3/g)**
#4	400	3.1	173	0.341
#5	800	2.4	149	0.237
#6	1200	2.3	154	0.266

*****above pore radius 1 nm

5.7 Silver doped silica particles

Nanosized commercial silica was decorated with silver particles. The Ag^+-ions were reduced by annealing at 400-900 ºC for 75 min in air. The X-ray diffractogram (Figure 24) reveals that Ag is present in the material. It is shown that the silver peak intensities change with annealing temperature, suggesting growth of silver particles or an increase in silver concentration.

The transmission electron micrographs also suggest Ag particle growth with increasing temperatures. Figure 25 displays the Ag/SiO_2 powders annealed at 700 ºC and 800 ºC. Figure 26 present the Ag/SiO_2 powder annealed at 900 ºC. A larger Ag particle size distribution is also presented. The Ag size distributions are summarized in Table 8. The samples annealed at 400-600 ºC are not included in the particle size measurements due to insufficient number of distinguishable Ag particles. XRD and HRTEM confirms the presence of Ag nanoparticles, it is thus suggested that the particle sizes are too small to be determined. The increasing particle size could suggest a growth mechanism such as Ostwald ripening, but no definite proof has been obtained in this study.

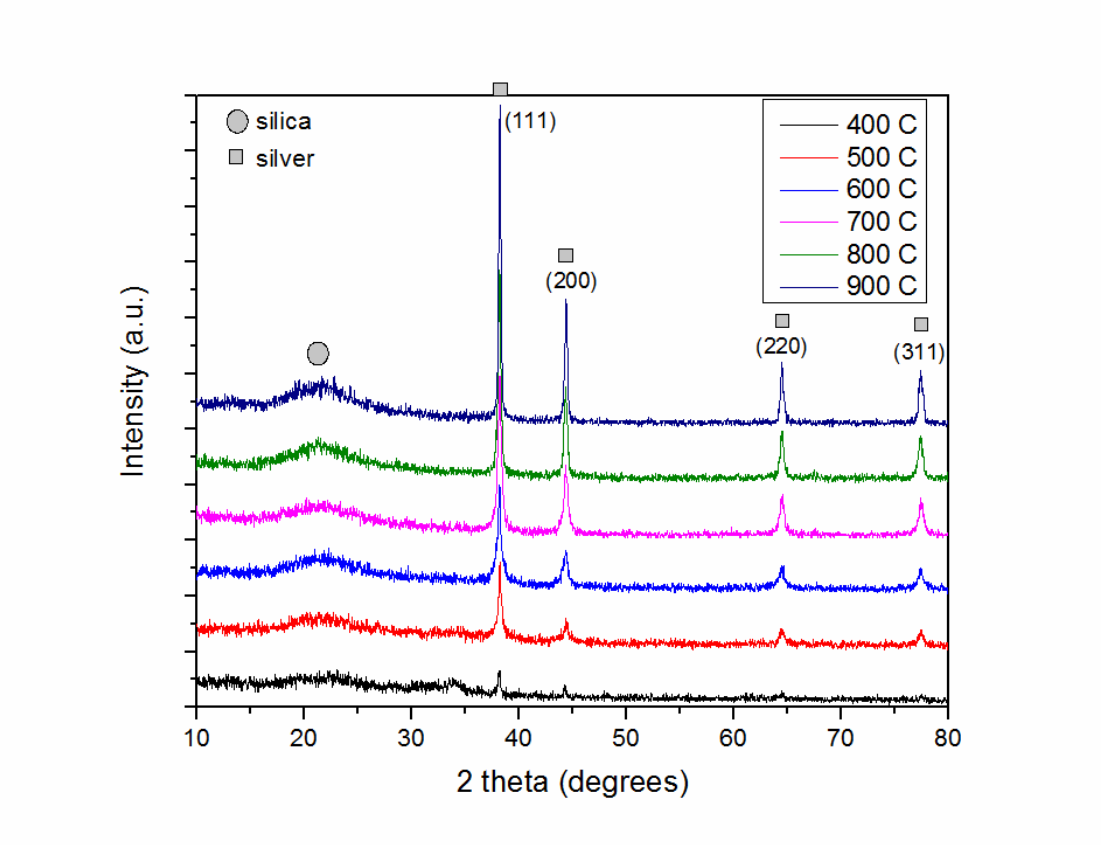

Figure 24. X-ray diffractogram of Ag/SiO_2 samples annealed at 400-900 ºC. The circle marks amorphous SiO2 and the squares are fcc Ag.

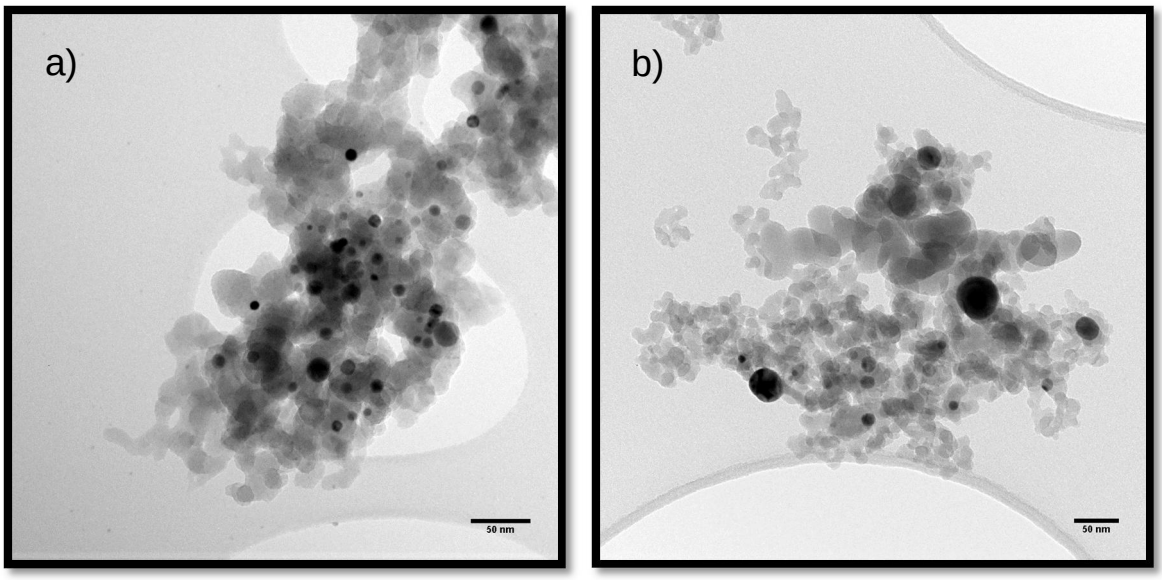

Figure 25. Transmission electron micrographs of Ag/SiO_2 samples annealed at a) 700 ºC and b) 800 ºC. Scale bars 50 nm.

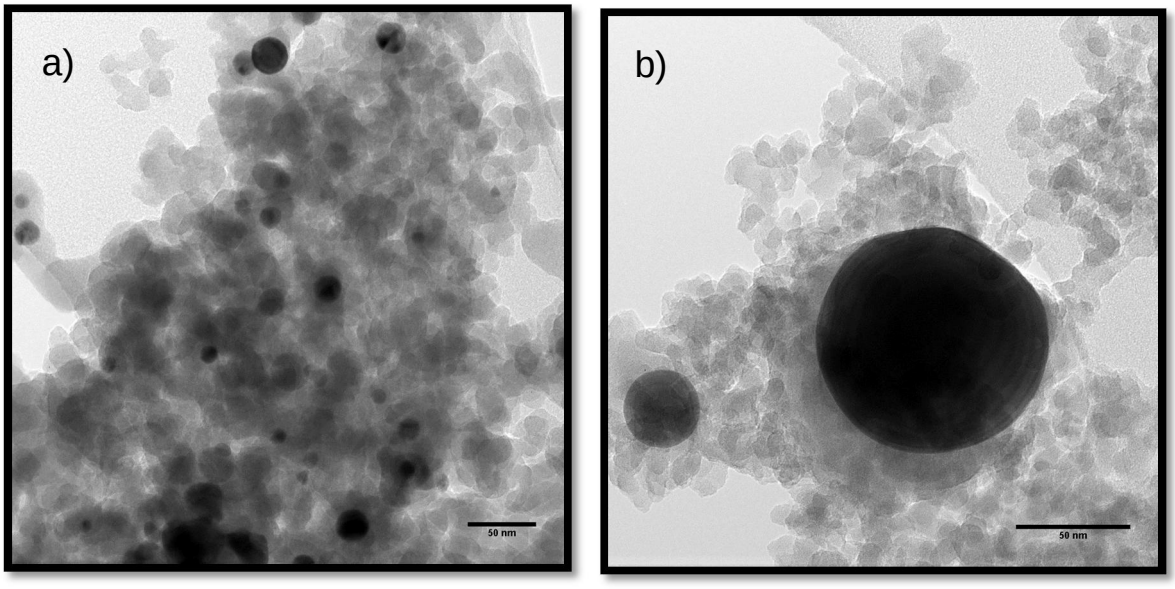

Figure 26. Transmission electron micrographs of Ag/SiO_2 samples annealed at 900 ºC. The size distribution of Ag nanoparticles is clearly observed in a) and b) showing larger Ag particles. Scale bars 50 nm.

Table 8. Ag size distributions for Ag/SiO_2 samples annealed at 700-900 ºC.

Annealing temperature	**700 ºC**	**800 ºC**	**900 ºC**
Average size	9.5 nm	19.9 nm	23.6 nm
Standard deviation	4.2 nm	12.1 nm	22.6 nm
Smallest particle size	5.8 nm	6.7 nm	8.8 nm
Largest particle size	21.8 nm	48.7 nm	101.9 nm

5.8 Characteristics and performance of fire-retardant coatings

The FR compositions were mainly tested using coatings with target dry film thicknesses (DFT) of 400 µm. The average values of measured DFT, expansion factor (EF) and maximum substrate temperature of the samples are presented in Table 9. Respectively, Average temperature developments of the samples and the effect of expansion factors on the maximum substrate temperature are visualised in Figure 27. The performances of the coatings filled with FRs fell between the commercial FR coating and the reference sample. Composition 1 with 50 wt% of APP-PER-MeI mixture was found to be most efficient of the compositions, at least when the DFT of coating was approximately 400 µm. Coating performance benefited from a high expansion factor, as it implies high porosity and char thickness.

Table 9. The maximum substrate temperatures (Tmax), dry film thicknesses (DFT) and expansion factors (EF) for the fire retarded UPR compositions tested.

Composition		**DFT (µm)**		**T_{max} (°C)**		**EF**	
Ref	No additives	400	±10	440	±20	-	
1	APP-PER-MeI (IFR)	390	±20	290	±20	18.5	±2.4
2	IFR+MH	410	±30	360	±60	11.7	±2.7
3	IFR+MH-SCS	410	±10	360	±30	9.3	±2.0
4	IFR+SiO_2	390	±20	330	±30	12.5	±2.2
5	IFR+SiO_2+MH	370	±40	380	±20	8.6	±1.4
6	IFR+GO	390	±20	340	±30	17.9	±1.5
7	IFR+MH-SCS+GO	400	±40	380	±30	13.2	±2.7

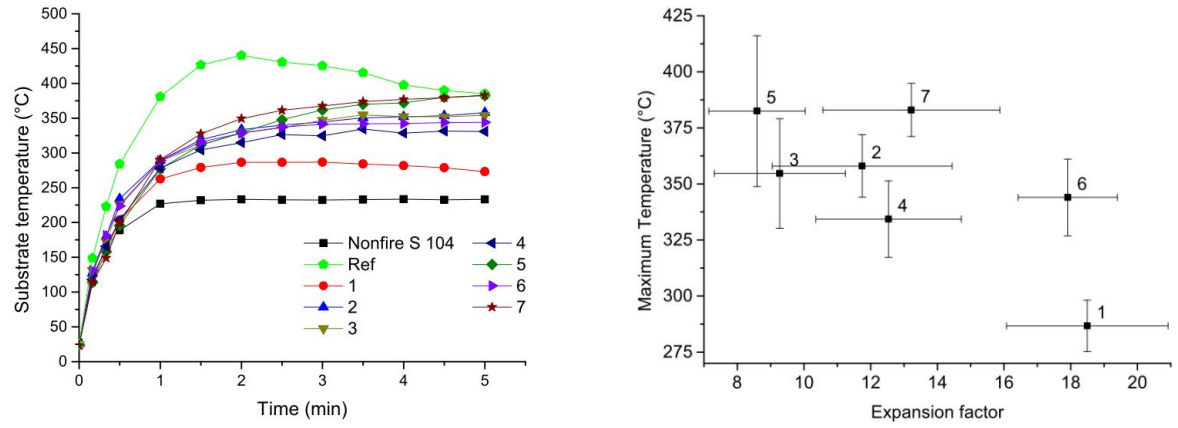

(a) (b)

Figure 27. (a) Time-temperature curves of all tested compositions with DFT of 400 µm. (b) Expansion factors and maximum substrate temperatures for said samples.

The temperature development of composition 1 is shown in Figure 28 (a). Due to the porous char clearly visible in Figure 28e, composition 1 provided significantly better thermal resistance to the sample than was the case for the reference sample seen in Figure 28f. However, composition 1 was inferior to the commercial IFR coating, probably due to its lower EF and large pore size.

The reason for the small expansion factor achieved with composition 1 coatings was probably insufficient melt viscosity of the coating. During a fire, the rheological properties of intumescent coatings are critical for their performance. The coating is required to be viscous enough to be able to trap evolving gas, but fluid enough for bubble growth to be possible. During the fire test, gas was observed escaping the coating through intense bubble disintegration. In the validation test run, slight bubbling of the commercial coating was observed in the initial moments of the test, which was followed by a long phase of smooth expansion. Addition of inorganic additives, such as MH-SCS, appeared to increase the melt viscosity of the pyrolysing coating, reducing the pore size of the expanded char. The char produced by composition 3 is presented in Figure 28g However, at least with DFT of ~400 µm, the resulting expansion factors were lower than the ones achieved with composition 1 (Figure 28b).

With high values of DFT, MH-SCS had a beneficial effect. It reduced the dripping of the coating, of which composition 1 suffered from. The expansion factors and maximum substrate temperatures were examined as a function of DFT. The expansion factor increased with DFT for both compositions. For composition 1, the expansion factor was more unpredictable, probably due to the low viscosity of the coating leading to a chaotic expansion process and dripping. It was found that with a DFT under 200 µm, expansion was insufficient for both coating compositions. Due to the high expansion factors they had, coatings with high DFTs should also have a high thermal resistance. However, maximum substrate temperature of the samples reduced after increasing the DFT above 500 µm. This may be attributed to the experimental setup. As thick coatings expanded, the char surface moved closer to the burner flame, increasing thermal flux into the sample. On the other hand, thermal radiation emitted by the samples reduced with substrate temperature, making further reduction of the maximum substrate temperature more difficult.

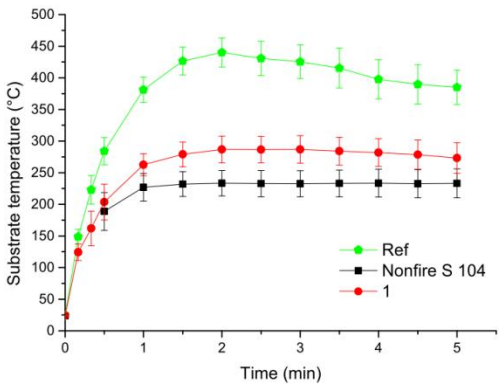

(a)

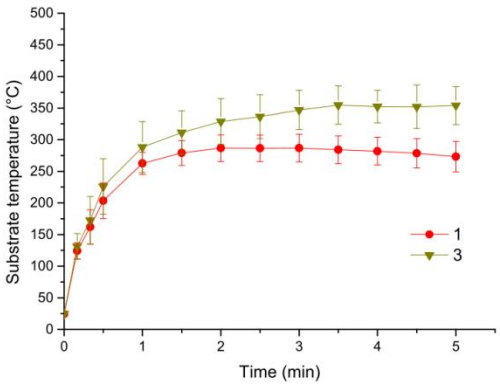

(b)

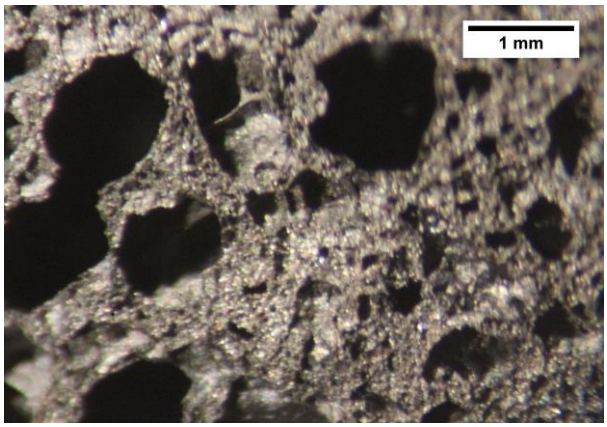

(c)

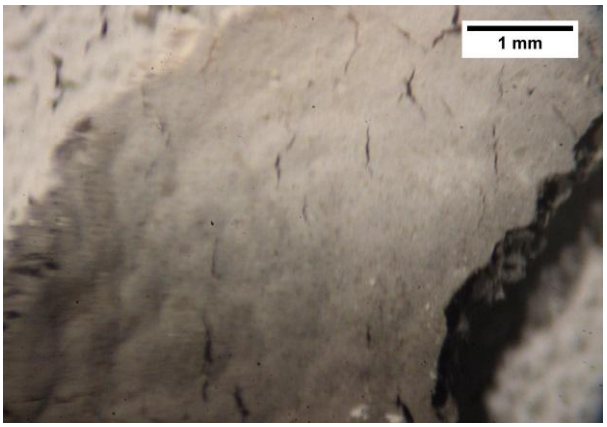

(d)

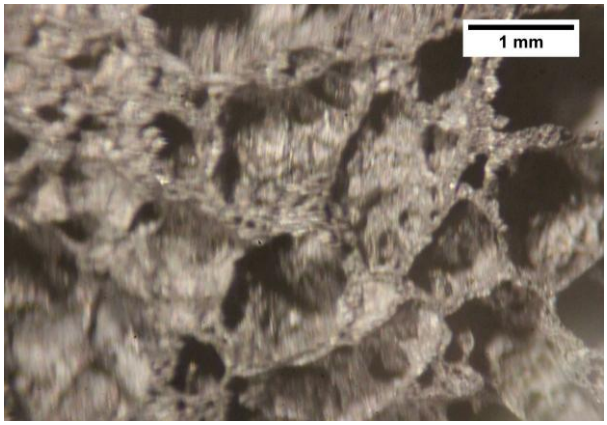

(e)

Figure 28. (a) Fire test results for composition 1 with 50 % APP-PER-Mel compared with unfilled UP coating and a commercial IFR coating. (b) Composition 3 with MH-SCS particles present provided thermal resistance inferior to composition 1. (c) Backside of the char layer produced by composition 1. (d) Backside of reference sample. (e) Backside of sample coated with composition 3.

6. Conclusions

Polymer and silica microcapsules were used to encapsulate various active agents including biocides, anti-foulant, fire-retardants and self-healing agents. Microcapsules with active agents were incorporated into paint and varnishes to demonstrate their functionality. In overall, a development platform was created for the microencapsulation technology. Moreover, promising coatings were developed with fire-retardant and self-healing performances.

To summarise the main findings, the results indicated that microencapsulation technology may prolong the usability of anti-fouling coatings. PS capsules were developed and further modified using PCL. The increase of hydrophilicity in the PS capsule using PCL had evidently effect on the release rate of IPBC. The IPBC release studies from the paint matrices to water indicated that IPBC is released faster from the paint matrix than from the lacquer matrix. This is due to the fact that the lacquer film was denser than the paint film. Indeed, microcapsules can improve the anti-moulding performance of one-component paints. However, further optimisation is needed to improve the release mechanism for two-component paints and varnishes.

Minor differences were revealed in the accelerated anti-fouling experiments. The aging accelerated the moulding on glass plates. The substrate is known to have effect on the mould growth on the coating. The mould growth was very slow on glass plates compared to as a birch veneer reference, where the surface was fully covered with the moulds after 6 weeks. After changing the new agar substrate at 18 weeks the mould index started to increase again.

Wood contains nutrients required for mould growth and thus, the aging tests were also performed on pine wood surfaces. The mould growth was faster on lacquer surfaces than on paint surfaces. Lacquer with synthetized capsule had best performance on aged wood surfaces. IPBC with or without encapsulation did not prevent mould growth on wood surfaces (aged or not aged) as efficiently as on glass plates. Only small mould growth was detected on paint samples. However, clear differences between paint samples containing suspended or encapsulated IPBC (MI 0-1) could not be found. Nevertheless, the microcapsules are expected to provide long-term release of active agent. Therefore, both accelerated and field tests are required for the feasibility testing.

The self-healing properties of the polyester coatings with and without PS-IPDI microcapsules were investigated. The coatings were scratched and the scratched areas were scanned to detect the evolving current over time. SVET (scanning vibrating electrode technique) showed positive trend in the first few hours for self-healing samples compared to reference sample. However, the effect was not observed at longer time period, probably due to cathodic delamination predominates over inhibition. This conclusion was supported by the LEIS (localized electrochemical impedance spectroscopy) results, where slight positive trend in self-healing samples was detected, whereas there was a negative trend in the reference.

The FR composition 50 wt% of APP-PER-Mel mixture was found to be most efficient of the compositions, when the thickness of coating layer was approximately 400 µm. The substrate temperatures behaved in a similar manner as in the screening test, with the temperature increasing to a maximum, after which it starts to decrease. The effect is probably due to a white product layer on the surface of the sample reflecting thermal radiation. However, no intumescence effects were observed with the tested silica / APP – polyester paint coatings in the cone calorimeter test.

7. Publication list

The publications in conferences, seminars, trade or scientific journals regarding to RESCOAT project:

- Q. Chen, J. Larismaa, A. Keski-Honkola, K. Vilonen, O. Söderberg, S.-P. Hannula, ”Effect of synthesis time on morphology of hollow porous silica microspheres”, presented in 20th International Baltic Conference Materials Engineering 2011, Lithuania, Kaunas, 27–28.10.2011

- Q. Chen, J. Larismaa, A. Keski-Honkola, K. Vilonen, O. Söderberg and S.-P. Hannula, "Effect of synthesis time on morphology of hollow porous silica microspheres," Materials Science (Medziagotyra), 18, 1, 2012.

- Q. Chen, M. Friman, K. Vilonen, S.-P. Hannula, The Control of Size and Surface Morphology of Silica Microspheres by Sol-Gel Emulsion Approach, ICTA 2012, Bangkok, Thailand.

- L. Makkonen, Ice adhesion – theory, measurements and countermeasures. Journal of Adhesion Science and Technology, 25, 2012, 33 p.

- L. Makkonen: Two presentations and a session chairmanship. Meeting of the International Advisory Committee of IWAIS. Invited lecture at Chongqing University. XIV International Workshop on Atmospheric Icing of Structures (IWAIS), 8-13 May 2011, Chongqing, China, State Key Lab of Power Transmission Equipment & System Security and New Technology.

- S. Virtanen, J. Pelto, J. Nikkola, Preparation of polystyrene microcapsules and encapsulation of 3-Iodo-2-propynyl N-butylcarbamate (IPBC), Junior Euromat 2012, Lausanne, Switzerland.

- J. Nikkola, Novel responsive coatings and surfaces utilizing encapsulation technologies, Tekes Functional Materials Summer Festival, 2012.

- J. Nikkola, Raising the performance of coatings with encapsulation technology, Tekes Functional Materials – Four Seasons 2013.

- J. Pelto, S. Virtanen, T. Munter, J. Larismaa, S. Jämsä, J. Nikkola, Encapsulation of 3-iodo-2-propynyl N-butylcarbamate (IPBC) in polystyrene-polycaprolactone (PS/PCL) blends, Journal of Microencapsulation, 4, 2014, 1-7.

- J. Nikkola, Microcapsule-protected actives reduce leaching, European Coatings Journal, 4/2014.

- H. Lipiäinen, The Effect of Various Additives on the Performance of an Unsaturated Polyester Coating as Fire Protection for Steel, M.Sc thesis, 88 p., Aalto University, 2014.